

AN ABSTRACT OF THE DISSERTATION OF

Tracy Arras for the degree of Doctor of Philosophy in Water Resources Engineering presented on March 27, 2014.

Title: A GIS Approach to Estimating Continuous Hydraulic Conductivity and Equivalent Hydraulic Conductivity.

Abstract approved: _____

Jonathan Istok

Estimating the hydraulic conductivity of earth materials is important for many water resource modeling efforts, including predicting the transport of pollutants in ground water, computing surface runoff for flood control, and computing water budgets. This research implicitly used topography, soil, and climate data to estimate plausible continuous hydraulic conductivity values at a basin-wide scale. The study demonstrated that continuous estimates of aquifer hydraulic conductivity using a geographic information system (GIS) approach are plausible. Manuscript 1 investigated the effects of different GIS stream generation methods on continuous estimates of conductivity and independent sources were used to verify the plausibility of the results ranging from well pumping tests to Soil Survey Geographic Database (SSURGO).

Because of the disparity between the scales at which measurements are taken for traditional conductivity estimates and those required for hydraulic and hydrologic modeling, conductivity point data are typically upscaled to the meter-to-kilometer scale and then referred to as equivalent conductivities. Manuscript 2 developed and tested a new method for computing basin-scale equivalent hydraulic conductivities and explored the relationships of catchment and drainage paths equivalent conductivities to a watershed's equivalent conductivity using GIS. Manuscript 3 investigated how the methodology of using GIS and landscape descriptors to estimate continuous hydraulic conductivity and equivalent conductivity are impacted by DEM resolution.

©Copyright by Tracy Arras
March 27, 2014
All Rights Reserved

A GIS Approach to Estimating Continuous Hydraulic Conductivity and
Equivalent Hydraulic Conductivity

by
Tracy Arras

A DISSERTATION

submitted to

Oregon State University

in partial fulfillment of
the requirements for the
degree of

Doctor of Philosophy

Presented March 27, 2014
Commencement June 2014

Doctor of Philosophy dissertation of Tracy Arras presented on March 27, 2014

APPROVED:

Major Professor representing Water Resources Engineering

Director of the Water Resources Graduate Program

Dean of the Graduate School

I understand that my dissertation will become part of the permanent collection of Oregon State University libraries. My signature below authorizes release of my dissertation to any reader upon request.

Tracy Arras, Author

ACKNOWLEDGEMENTS

My sincere appreciation is given to Jack Isok because without his guidance, support and belief in me this dissertation would not exist. Many, many, thanks!

This dissertation is in dedication to Marie Arras, my mother, best friend, and my dearest love.

I would like to thank Oregon Department of Geology and Mineral Industries for use of the LiDAR DEMs used in this study.

TABLE OF CONTENTS

	<u>Page</u>
1. Introduction.....	1
2. A GIS Approach for Estimating Continuous Hydraulic Conductivity.....	3
Abstract.....	3
Introduction.....	3
Site Description.....	6
Methods.....	7
Results.....	11
Discussion and Conclusions.....	17
Literature Cited.....	19
3. Equivalent Basin-Scale Hydraulic Conductivity: A GIS Approach.....	22
Abstract.....	22
Introduction.....	22
Site Description.....	26
Methods.....	27
Results.....	32
Discussion.....	38
Conclusion.....	39
Literature Cited.....	40
4. The Influence of DEM Resolution on Hydraulic Conductivity Values.....	42
Abstract.....	42
Introduction.....	42
Site Description.....	44
Methods.....	44

TABLE OF CONTENTS (Continued)

	<u>Page</u>
Results	47
Discussion	56
Conclusion	57
Literature Cited	58
5. Conclusion	61
Literature Cited	62
6. Bibliography	63

LIST OF FIGURES

<u>Figure</u>	<u>Page</u>
Figure 2.1. Definition of parameters for equation 4.....	5
Figure 2.2 Delineated streams from different algorithms	11
Figure 2.3. Estimated K (m/day) values for Oak Creek watershed for each of the different stream delineation algorithms.	13
Figure 2.4. Published Krep (m/day) SSURGO soil data, interpolated K (m/day) estimates from pumping tests, and pumping locations. Red pumping symbols represent low K values, which are located by Oak Creek Stream and low K soil.	15
Figure 2.5. Single catchment with streams and K (m/day) from GIS different methods. Similar drainage density for all methods except ~USGS and Peucker Douglas 1-7. Thematically mapped with quartile, 10 classes (equal distribution of cells in each class).....	16
Figure 3.1. Flow parallel to layering: the equivalent conductivity is the weighted arithmetic mean of the individual layer values.	23
Figure 3.2. Flow perpendicular to layering: the equivalent K (L/T) is the weighted harmonic mean of the individual layer values.	24
Figure 3.3. Continuous K (m/day) estimates from Geomorphologic-GIS method using a USGS 10 meter DEM. K ranges from 0.01-18 m/day. Dark blue represents the largest values of K, orange are mid values and yellow, lowest values, respectively. Drainage paths are overlaid in blue.....	29
Figure 3.4. Illustration of raster flow directions and corresponding lengths used to calculate equivalent conductivity. The cell size is 1; horizontal length is 1 unit and length along the diagonal is $\sqrt{2}$ units.....	30
Figure 3.5. New Kequiv (L/T) for drainage paths and areas.	32
Figure 3.6. Catchment equivalent conductivity (m/day) estimated using the different approaches: Kequiv _{dp} , Kequiva, K _G and K _A for each of the 54 catchments. Catchment numbers 1-26 represent the upper catchments of the watershed.	35

LIST OF FIGURES (Continued)

<u>Figure</u>	<u>Page</u>
Figure 3.7. Catchment equivalent conductivity (m/day) estimated using the different approaches: $K_{equiv_{dp}}$, K_{equiv_a} , K_G and K_A for each of the 54 catchments. 28-53 represent the lower catchments of the watershed.	36
Figure 3.8. Equivalent conductivities along Oak Creek drainage path using the method of $K_{equiv_{mdp}}$ and equivalent conductivities of 12 catchments along Oak Creek drainage path using the method of K_{equiv_a}	36
Figure 4.1. K_{equiv} , harmonic approach.....	46
Figure 4.2. Oak Creek watershed study area, location of pumping tests, stream gage, and transects.	48
Figure 4.3. Channel cross-sections and tables showing difference between 1 m LiDAR DEM and coarsened 10, 20, and 30 m DEMs for lower, middle and upper transects.	49
Figure 4.4. Averaged catchment channel depth statistics for 1 m LiDAR DEM, coarsened 10 m, 20 m, and 30 m DEMs (after the Black Hat Transformation).	51
Figure 4.5. Cell values for BHT processed layers (ft), for: a. 1 m LiDAR DEM, b. 10 m DEM, c. 20 m DEM, and d. 30 m DEM. The numbers in the table correspond to the small rectangle shown in the center of each panel.....	52
Figure 4.6. Hillshade of BHT channel depth (small test area). Top left image is 1 m LiDAR DEM; top right, 10 m DEM; bottom left, 20 M DEM; and bottom right, 30 m DEM.	53

LIST OF TABLES

<u>Table</u>	<u>Page</u>
Table 2.1. Stream delineation algorithms, criteria, and parameters.....	8
Table 2.2. Estimated infiltration percentages by soil texture classification from Lou and Pederson, 2012.	9
Table 2.3. SSURGO, Krep classes and range of K.....	9
Table 2.4. Descriptive statistics for the stream delineation algorithms.....	12
Table 2.5. K (m/day) estimates at well locations for SSURGO Soil data, pumping tests and GIS methods.....	14
Table 2.6. Comparison of K estimates for small test catchment shown in figure 2.6.....	17
Table 3.1. Estimated infiltration percentage by soil texture classification (Lou and Pederson, 2012).	28
Table 3.2. Equivalent hydraulic conductivities (m/day) and differences.....	33
Table 3.3. Catchment descriptive statistics for equivalent conductivities (m/day): K_A , K_G , K_{equiv} , $K_{equivdp}$, and $K_{equivmdp}$	37
Table 3.4. Equivalent conductivity value for Oak Creek watershed	37
Table 4.1 Watershed DEM statistics, feet.	47
Table 4.2. Descriptive Statistics of K for Oak Creek watershed across resolutions.	53
Table 4.3. K (m/day) estimates at pumping test locations and Surfleet’s stream gage: soil survey data, pumping tests and the calculated K from this study.....	54
Table 4.4. Conductivity (m/day) differences between soil survey, Krep, and the study’s values at different DEM resolutions.....	55
Table 4.5. Conductivity differences between pumping tests and the study’s values at different DEM resolutions, m/day.....	55
Table 4.6. Equivalent conductivity (K_{equiv}), m/day for Oak Creek Watershed.	56

1. Introduction

Estimating the hydraulic conductivity of earth materials is important for many water resource modeling efforts, including predicting the transport of pollutants in ground water, computing surface runoff for flood control, and computing water budgets. Hydraulic conductivity can be experimentally determined in the laboratory using constant-head and falling-head permeameter tests and in the field using slug tests, pumping tests, and related methods (Domenico and Schwartz, 1990). Laboratory methods require core samples, which are time consuming and expensive to collect, and are subject to various sampling and testing artifacts. Field measurements are desirable but expensive and typically sparse. Both field and laboratory methods provide point estimates of hydraulic conductivity and are subject to various scaling problems when discretized across an entire basin.

This research implicitly used topography, soil and climate from readily available data to estimate plausible continuous hydraulic conductivity values at a basin-wide scale. The study demonstrated that continuous estimates of aquifer hydraulic conductivity using a geographic information system (GIS) approach are plausible. Manuscript 1 investigated the effects of different GIS stream generation methods on continuous estimates of conductivity and independent sources were used to verify the plausibility of the results ranging from well pumping tests to representative conductivity (Krep) values in the Soil Survey Geographic Database (SSURGO).

Because of the disparity between the scales at which measurements are taken for traditional conductivity estimates and those required for hydrologic modeling, conductivity point data are typically upscaled to the meter-to-kilometer scale and then referred to as equivalent conductivities. The usage of the term *equivalent* reflects the fact that hydraulic conductivity is not an additive variable. Even though upscaling has been studied intensively, most work has focused on synthetic data sets, or otherwise idealized conditions (e.g., uniform layering, infinite spatial extents, and logarithm normal distribution) with known parameters, etc. Application of these techniques to real aquifer systems has been more limited. In particular, little work has been done on evaluating upscaling techniques for large natural watersheds, which are irregular in shape, finite in extent, and heterogeneous. The use of upscaling methods to estimate the equivalent hydraulic conductivity of a natural watershed has not been extensively studied. It is not well understood how to incorporate the geomorphology of the watershed (stream density, drainage paths, slope, etc.) into upscaling techniques. The objective of manuscript 2 was to develop and test a new method for computing basin-scale equivalent hydraulic conductivities for

use in hydrologic modeling and to explore the relationships of catchment and drainage path equivalent conductivities to a watershed's equivalent conductivity using GIS.

Over the last three decades, many authors have shown that increasing DEM resolution strongly influences computed hydrologic parameters. The majority of these studies have been conducted with 10 m and greater USGS DEMs and low-altitude aerial photography. Only recently have studies started to evaluate the utility of high-resolution DEMs obtained from airborne Light Detection and Ranging (LIDAR) for hydrologic investigations. The objective of manuscript 3 was to investigate for the first time how continuous hydraulic conductivity values and equivalent conductivity values estimated with GIS are affected by LiDAR DEM resolution.

The original research conducted in this dissertation contributes a new body of knowledge in the science of hydrology and GIS. Manuscript 1 demonstrated that the selection of stream density strongly impacts calculated conductivity values, while the robustness of the stream delineation method is not critical. Regardless, of the stream delineation method selected all methods produced plausible conductivity estimates when compared to local pumping tests and soil survey data. Manuscript 2 used GIS to estimate equivalent conductivities for the first time using both a raster and vector approach; and uniquely investigated using only drainage path cells to calculate a catchment's and watershed's equivalent conductivity value. The conclusion of Manuscript 2 indicates equivalent conductivity can be calculated from drainage paths in a catchment or watershed as long as conductivities values in the drainage paths are representative of the hydrologic area. Manuscript 3 demonstrated that a 10 m DEM resolution is optimal when using GIS and landscape descriptors to estimate continuous conductivities and equivalent conductivities, when compared to 20 and 30 m DEM resolutions. While 20 and 30 m DEM resolutions appear suitable for these analyses there are underlying problems with accurate representation of channel depth and width with coarser DEMs. Because of the fine topography detail in the 1 m DEM, the continuous conductivity values and equivalent conductivity values are larger than the continuous values in 10 m DEM and further research needs to be conducted to determine whether the 1 or 10 m DEM is optimal for estimating conductivity and equivalent conductivity with GIS.

2. A GIS Approach for Estimating Continuous Hydraulic Conductivity

Abstract

Drainage patterns often are influenced by groundwater systems and this study implicitly used topography, soil and climate data to estimate plausible continuous hydraulic conductivity at a basin-wide scale. The study demonstrated the effect of different stream generation methods on continuous basin-scale estimates of aquifer hydraulic conductivity using a GIS approach. Independent sources were used to verify the plausibility of the results ranging from well pumping tests to SSURGO soil survey data. By using the strengths of GIS with the best data available, we can increase the effectiveness of our estimates of continuous K.

Introduction

The coupling of geographic information systems (GIS) with hydrological applications emerged in the late 1980s (Goodchild et al., 1992; Fotheringham and Rogerson, 1994). Today, numerous hydrologic modeling techniques employ GIS, and range from simple data compilation and management to sophisticated modeling and simulation. A review of these modeling techniques and applications can be found in Maidment, 1993; Goodchild et al., 1996; McDonnell, 1996; and Gurnell and Montgomery, 2000. One recent research area is the use of GIS to estimate basin-scale heterogeneity in aquifer hydrologic properties (Refsgaard et al., 2010). Accurate estimation of hydraulic conductivity is important for aquifer characterization, modeling groundwater flow and solute transport, and management of groundwater resources.

Hydraulic conductivity is known to be a highly-spatially variable and can vary both horizontally and vertically (Guta et al, 2006). It is strongly influenced by rock and soil forming processes acting over geologic time scales. Hydraulic conductivity is a measure of a material's capacity to transmit water. It is defined using Darcy's Law:

$$q = -K \frac{dh}{dl} \quad (1)$$

where q [LT^{-1}] is the volumetric groundwater flow rate per unit area (or flux); K [LT^{-1}] is the hydraulic conductivity; and dh/dl is the hydraulic gradient along the flow direction l .

Hydraulic conductivity can be experimentally determined in the laboratory using constant-head and falling-head permeameter tests and in the field using slug tests, pumping tests, and related methods (Domenico and Schwartz, 1990). Laboratory methods require core samples, which are time consuming and expensive to collect, and are subject to various sampling and testing artifacts. Field measurements are desirable but expensive and typically sparse. Both field and laboratory methods provide point estimates of hydraulic conductivity and are subject to various scaling problems when discretized across an entire basin. Conventional interpolation methods, such as kriging have been used to estimate continuous basin-scale values of hydraulic conductivity and while these methods are valuable they lack the utilization of landscape data such as slope, drainage density and groundwater depth. The interaction between topography, surface water, and aquifer properties have long been recognized but literature is limited on hydraulic conductivity studies that incorporate geomorphology (Lou and Pederson, 2011).

Another approach for estimating hydraulic conductivity at the basin scale involves developing correlations between hydraulic conductivity and more widely measured physical properties (Rawls et al., 1992; Hillel, 1998; Campbell, 1974; Brooks and Corey, 1964; and Van Genuchten, 1980). Many studies propose empirical relationships between hydraulic conductivity and soil water characteristics, particle size distribution and soil texture. Recent studies involve multiple descriptors and utilize statistical correlations that include techniques such as, neural networks, decision trees, and pedotransfer functions (Lagacherie, et al. 2007). Current methods are also adopting a combination of methods with the fusion of remotely sensed data. While there seems to be a strong use of soil descriptors, which are limited to sample locations or government published soil survey data, most methods are not incorporating geomorphic characteristics.

Lou et al. (2008, 2010, 2011) proposed methods to estimate hydraulic conductivity based on surface topography, flow path distances, recharge and aquifer thickness under the following assumptions: 1) the aquifer is effectively drained and under steady-state dynamic equilibrium through the interaction of surface water, groundwater and topography (valley network formation has concluded and drainage density is stable) and 2) groundwater flow is described by Darcy's Law, and the DuPuit-Forchheimer assumptions that the aquifer is unconfined and flow is primarily horizontal apply (Lou et al, 2011). The discharge per unit length ($u = 1$) of the channel, q' [L^2T^{-1}]

$$q' = \frac{1}{2}K \left(\frac{H^2 - (H - d)^2}{W} \right) \quad (2)$$

Under dynamic equilibrium conditions, q' can be estimated from recharge, R , which equals annual precipitation multiplied by infiltration percentage.

$$q' = R * (2Wu) / u = 2RW \quad (3)$$

Rearranging the equations

$$K = \frac{4W^2R}{[H^2 - (H - d)^2]} \quad (4)$$

Where K is the hydraulic conductivity [L/T]; W is the length of effective groundwater drainage [L]; R is the recharge rate [L/T]; d is the valley depth from channel water level [L]; and H is aquifer thickness [L] (figure 2.1).

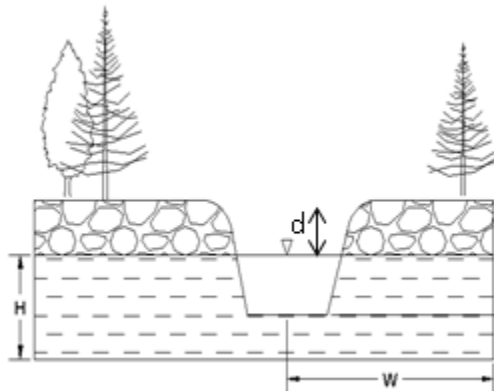


Figure 2.1. Definition of parameters for equation 4.

Valley formation starts with precipitation at the surface. As the precipitation infiltrates into the ground it leads to depressions and weathers and erodes the underlying soil. Large storms also induce erosion and valley formations. Overtime the process is repeated until valleys are formed and equilibrium is obtained between the groundwater flow and recharge of the surface.

At this point valley formation stops, steady-state dynamic equilibrium is achieved and drainage density is established and stable. The water table elevation is unlikely to reach the topographic surface at the watershed divide but it is reasonable to assume this elevation represents an approximation of the water table elevation at the watershed divide (Lou et al, 2011).

Delineating drainage networks using digital elevation models has only been possible within the last two decades. Several proven algorithms exist to create stream networks from digital elevation models (Montgomery 1989, 1992; Tarboton, 1997; Tarboton and Ames, 2001; Tucker et al., 2001). In this study several stream generation algorithms were investigated and used to evaluate the plausibility of estimating continuous hydraulic conductivity through surface drainage patterns. It was hypothesized that a discretized (grid) basin-scale predictive model of hydraulic conductivity could be developed with any of the stream network algorithms. To test this hypothesis LiDAR DEMs and GIS were coupled together to compile a continuous model of hydraulic conductivity through delineation of high-resolution surface drainage patterns. The overall objective was to determine if continuous hydraulic conductivity values could be estimated using drainage patterns in a mountainous forested watershed, and, if so, to determine the effect of stream delineation method on continuous hydraulic conductivity estimates? Modeled estimates were compared to soil survey data from USDA and to estimates obtained from a limited number of field pumping tests.

Site Description

The study used a small catchment in the Upper Willamette 8-digit Hydrologic Unit Code (17090003) subbasin, and is located in Benton County east of the Coast Range and west of the Cascade Range. The Upper Willamette watershed is representative of the other Willamette basin watersheds (Yamhill, Tualatin, Middle Willamette, etc.) with respect to soils, topography, precipitation and climate. Oak Creek watershed is located in the McDonald/Dunn Research Forest managed by the College of Forestry, Oregon State University. The watershed is approximately 3360 hectares; elevations range from 60 to more than 585 meters. The average annual precipitation for 1971-2000 was 137 cm/yr with a range of 107-188 cm/yr. Precipitation in the watershed is predominantly rain. The underlying bedrock, the Siletz River Volcanics, is a basalt formation. The most common surface soil texture is silty clay loam, although some silty loam is also present. The forest trees are predominantly Douglas-fir with minor components of other conifers, hardwood species, and grassy meadows.

Methods

2010 LiDAR DEM was used for the delineation of Oak Creek's stream network and watersheds; for parameter estimation of effective drainage length, W ; and valley depth, d . LiDAR DEM data were obtained from Oregon Department of Geology and Mineral Industries in ESRI grid format with 3 foot resolution and vertical accuracy is 0.67 feet. Stream networks were compiled from LiDAR DEM using the following stream generation algorithms: Strahler Stream Order, Length-Area, Peuker Douglas, and a manually assigned stream threshold based on drop analysis (Tarboton, and Ames, 2001; Tucker, et al., 2001, McDonnell, 1996; Montgomery, and Dietrich, 1992). In addition, a manually assigned large stream threshold was used to generate a stream network similar to USGS 1:24,000 stream networks.

Stream generation algorithms in this study assigned flow directions based on the 8-cardinal directions (N, S, SW, etc.), known as the D8 method (Tarboton and Ames, 2001). The Strahler stream order algorithm evaluates grid cells that have other cells draining into them and the order of inflowing cells is used to determine the stream order according to Strahler order rules (Tarboton and Ames, 2001). The Length-Area method evaluates the longest upstream path length and uses the D8 contributing area as a threshold with stream length as stated by Hack's Law (relationship between length of streams and area of watershed, $L \sim A^{0.6}$, Area – ML^y) (Rigon, et al., 1996). Peuker Douglas (Peuker and Douglas, 1975), a morphology based algorithm, identifies valley form from concavity of cells (upward curved grid cells that reflect a flow dissection pattern). And the manually assigned stream threshold incorporates drop analysis to objectively select the highest resolution stream network that obeys the stream drop law. The stream drop law evaluates the mean stream drop in elevation for 1st order streams and compares it to higher stream orders. If statistically different then the stream network does not obey the drop law. A T-test was used to aid in finding the smallest threshold where the absolute value <2 for the drop analysis was achieved.

Approximately the same drainage density ($9.42 \times 10^{-3} \text{ m}^{-1}$) was achieved for each stream delineation method and two completely different drainage densities were also compiled for comparison in the study; a lower drainage density ($1.86 \times 10^{-3} \text{ m}^{-1}$), representative of a USGS 1:24,000 stream network, and a much higher drainage density ($3.14 \times 10^{-2} \text{ m}^{-1}$). Table 2.1 provides an overview of the stream delineation algorithms used in this study.

Table 2.1. Stream delineation algorithms, criteria, and parameters.

Methods	Criterion and Parameters
Strahler Stream Order	D8, stream order 7-12
Length-Area	D8, ML^y ; $M = 0.01$, $y = 1.25$
Peuker Douglas, 1-7 (high drainage density) Peuker Douglas, 3-7	D8, weight center, side and diagonal: 0.4, 0.1, 0.05 with drop analysis. Stream orders 1-7 and 3-7 were used
Stream Threshold by Drop Analysis	D8, smallest stream threshold value of 1104 was used
Stream Threshold to simulate USGS 1:24,000 Stream network (low drainage density)	D8, threshold of 11,970 cells were used to generate stream origination

Aquifer thickness, H , was assumed constant ($H = 98.4\text{m}$), based on estimates ranging from 65 to 131 meters obtained from USGS Scientific Investigations Report 2005-5168. The valley depth, d , was calculated with a Black Top Hat (BTH) transformation with a moving neighborhood radius of 4 cells, determined by associating results from different radii with manually measured depths (Rodrigues et al., 2002; Lou and Pederson, 2012). Briefly, an incision surface was created with a roving window that acts as a filter to extract maximum elevations or peaks within each window. This process is called dilation. Then a similar process is repeated with the dilation surface to extract low elevations or channels. This results in a closing surface. Valley depths are determined by subtracting the LiDAR DEM from the closing surface and averaged over the catchment area. The term catchment is used instead of watershed to represent smaller drainage areas that are within Oak Creek watershed.

Colon and others (2005) estimated groundwater recharge to be 40.6-50.8 cm per year for the study area, noting higher elevations have increased precipitation and increased recharge. Lee and Risley (2002) estimated the mean annual recharge for the study area to range from 25.4-38.1 cm. In this study, spatially varying recharge, R , was estimated from precipitation and soil data (also spatially varying).

$$R = (\text{Precipitation}) (\text{Infiltration Percentage}) \quad (5)$$

The 30-year (1971–2000) spatially variable mean annual precipitation data were obtained from Oregon State University, PRISM Climate Group and ranged from 108 to 187 cm per year. Soil Survey Geographic Database (SSURGO) was obtained from USDA-NRCS, which was assigned an infiltration percentage based on soil texture classification (Table 2.2) (Lou and Pederson, 2012). Using the assigned soil infiltration percentage values and the precipitation, the calculated spatially variable mean annual recharge of Oak Creek watershed ranged from 0.13 to

28.96 cm. This method of estimating recharge implicitly takes into consideration the spatial variability due to climate, soil, vegetation, and topography (Lou and Pederson, 2012).

Table 2.2. Estimated infiltration percentages by soil texture classification from Lou and Pederson, 2012.

Soil Texture Classification	Estimated Infiltration Percentage
Unweathered Bedrock	0.1
Clay	0.2
Weathered Bedrock	1
Silty Clay	2
Gravelly Clay	3
Paragravelly Clay	3
Loam	5
Silty clay loam	5.5
Silty Loam	8.5
Very Cobbly Loam	15.5
Very Paragravelly Loam	15.5

The length of effective groundwater drainage, W , is the distance from any point in the catchment to the nearest stream moving downslope according to the D8 flow model. All parameters were averaged over each catchment before calculating hydraulic conductivity with Equation 4.

The study's conductivity values were compared to representative hydraulic conductivity estimates (Krep) from the soil survey 2009 database. The United States Department of Agriculture, Natural Resources Conservation Service provides soil data of the United States, which are produced by observation of ancillary data (aerial photography, geology, vegetation, etc.) and soil characteristics. Soil attributes are incorporated into an implicit conceptual model that is used to infer soil variation and is applied to predict soil variation at unobserved sites. Soil survey estimates of hydraulic conductivity are based on bulk densities (low, medium, and high) and soil texture, which are then categorized into one of the six defined classes shown in Table 2.3. A single Krep value is assigned to each soil unit.

Table 2.3. SSURGO, Krep classes and range of K

SSURGO Hydraulic conductivity Class	Krep Range, $\mu\text{m}/\text{sec}$
Very high	100 or more
High	10 to 100
Moderately high	1 to 10
Moderately low	0.1 to 1
Low	0.01 to 0.1
Very low	less than 0.01

As another check on the model's plausibility, conductivity values were calculated using pumping test data from 14 published well logs and the Theis equation (McElwee, 1980)

$$T = \frac{QW(u)}{4\pi s} \quad (6)$$

$$u = \frac{r^2 S}{4Tt} \quad (7)$$

where T is transmissivity [L^2/T]; Q is the pumping rate of the well [L^3/T]; s is well drawn down (change in hydraulic head measured from the beginning of the test) [L]; W(u) is the well function; r is the well radius [L]; S is storativity [unitless]; and t is time [T] measured from the beginning of the pumping test.

$$W(u) = -0.577216 - \ln(u) + u - \frac{u^2}{2 \times 2!} + \frac{u^3}{3 \times 3!} - \frac{u^4}{4 \times 4!} + \dots \quad (8)$$

This form of inverse modeling was used to find the average T and S values near the pumping well using data collected during the aquifer test. Measured well log data provided observed values for s, r, t, and Q and values of T and S were obtained by a best fit method. Once the best solution for T was found, hydraulic conductivity was computed

$$K = \frac{T}{b} \quad (9)$$

where b is the aquifer thickness [L].

Pumping test data were obtained from the State of Oregon, Water Resources Department. Pumping tests that were within the Oak Creek watershed and with documented b, Q and t were used in the calculation of hydraulic conductivity and compared to the study's hydraulic conductivity computed with GIS. The positional location of each pumping site was taken from Miles' (Miles, MS, Thesis, 2011) GIS database. Miles geo-located each pumping test site using latitude and longitudinal coordinates, street addresses, and surveying information from the State of Oregon, Water Resources Department, Well Log Query database, and Oregon's Explorer 0.5 m orthophotography. The positional accuracy of pumping test locations was estimated by Miles to be within a few meters. A 10 meter buffer was created around each

pumping site and conductivity values from GIS modeling were averaged within this buffered region to compare to conductivity values derived from the pumping test data.

The K estimates based on pumping test data fundamentally represent the horizontal K of the well screened layer (layer with highest production rate) and not the K of the entire saturated thickness which is what the GIS method estimates. K estimated by pumping tests represents a subset of K calculated with the GIS method. Even though K estimates from pumping tests and the GIS method are not directly comparable to each other they do indicate the plausibility of the GIS estimates.

Results

The Strahler stream order 3-7, Length Area, Peuker Douglas with stream order 7-12 and manual stream delineation by threshold all estimated similar numbers of streams and catchments (Fig. 2.2).

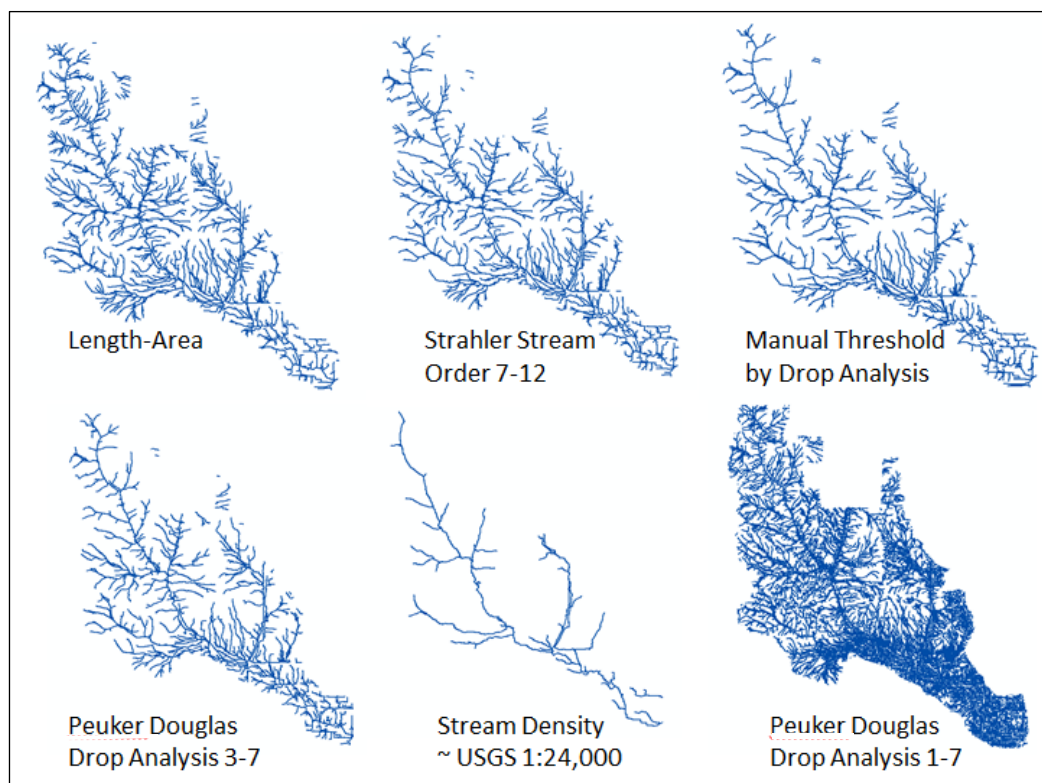


Figure 2.2 Delineated streams from different algorithms

The range and spatial distributions of estimated K values were also generally similar (Table 2.4). The Peuker Douglas with stream order 1-7 (larger drainage density), produced a smaller range of K values and the approximated 1:24K stream network estimated K values with a larger

range (because of a smaller drainage density), mean and standard deviation. An overall summary of the descriptive statistics from the various stream generation methods is presented in table 2.4 and the graphical results of estimated conductivity values for Oak Creek watershed are shown in figure 2.3.

Table 2.4. Descriptive statistics for the stream delineation algorithms.

Parameter Values	Manual Threshold	Length Area	Strahler Order 7-12	Peuker Douglas Order 3-7	~ USGS 1:24k	Peuker Douglas Order 1- 7
No. streams	1005	1573	1174	2552	196	51892
Categorical Drainage Density	Average	Average	Average	Average	Low	High
No. of catchments	1817	3371	2185	1994	157	42567
channel depth, d (m), averaged by catchment	0.03-0.97	0.03-0.76	0.03-1.16	0.03-1.16	0.03-0.52	0.03-1.37
W (km), distance to stream, averaged by catchment	0-6.7	0-5.8	0-9.8	0-10	0.05-15.4	0-5
K, (m/day) – range for all catchments	0-108	0-147	0-143	0-143	0.00061-379	0-7
K, (m/day) – mean for all catchments	4.6	3.3	3.9	4.9	45.7	0.6
K, (m/day) - standard deviation for all catchments	7.6	7.0	8.2	8.8	63.7	1.5

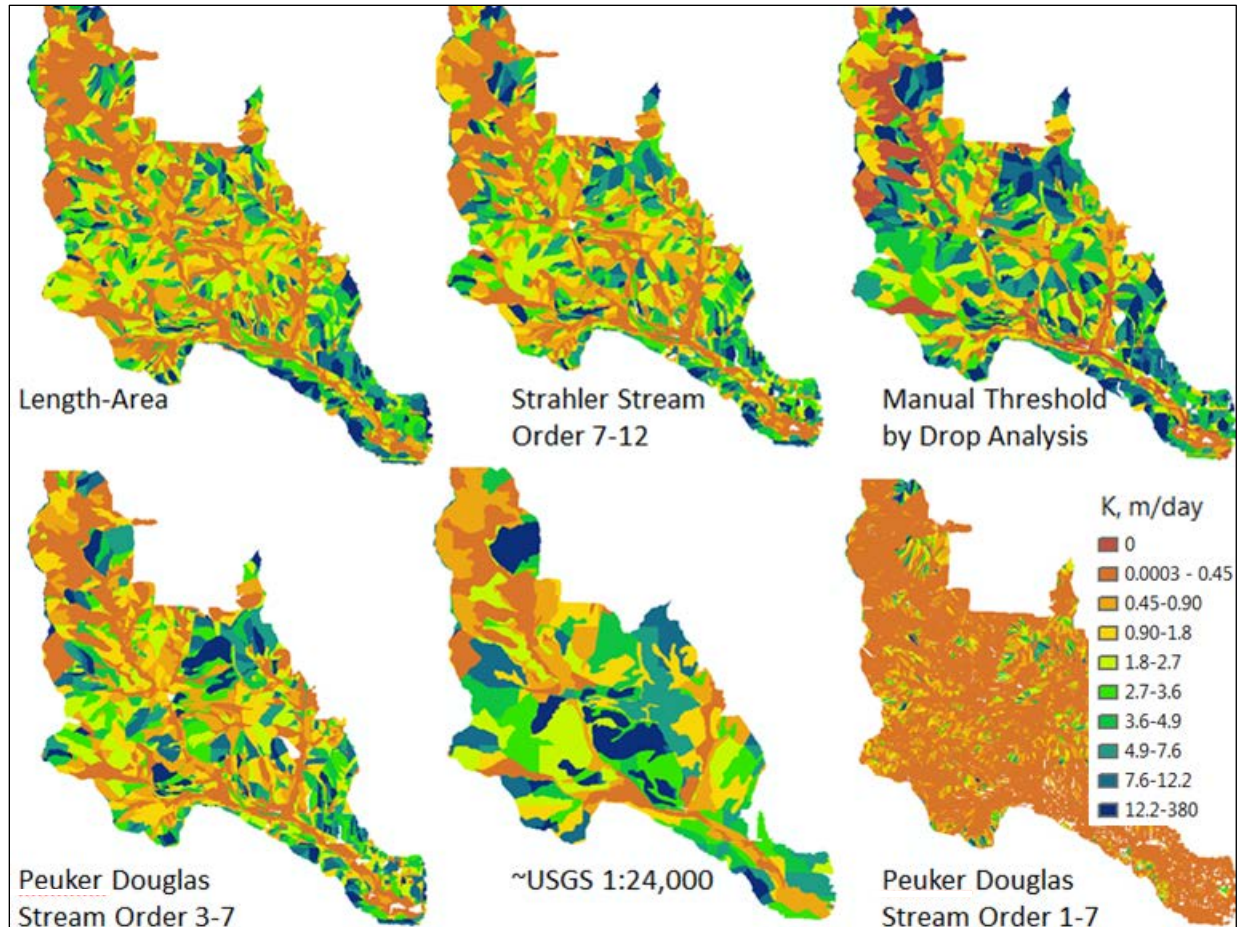


Figure 2.3. Estimated K (m/day) values for Oak Creek watershed for each of the different stream delineation algorithms.

The reduction of stream density and corresponding reduced number of catchments increases the distance of overland flow to the nearest stream and reduces the averaged channel depth over larger catchments resulting in larger estimates of K. Similarly, increasing the stream density reduces the overland flow distances; averages channel depth over smaller areas, and results in smaller K estimates. The estimates of K are not sensitive to the robustness of the stream delineation algorithm, but stream density is a key factor in the estimation of K. From this research it appears that most standard stream generation algorithms will provide similar results.

The high resolution DEM identifies the edge of some roads and categorizes them as streams. While these areas route stormwater runoff they were not created in a geologic process and therefore are not valid for use in estimating K. The stream network representing the 24K was derived from the 3-ft DEM and the stream threshold was reduced to replicate the 24K network. As a result, the 24K network also has some roads identified as streams. The original

USGS 1:24k stream network is based on a 30 meter DEM and was not used to be consistent on cell size.

Table 2.5 compares K values at the pumping test locations with those from the soil survey and the various stream delineation methods. K estimates from the soil survey, which are based on bulk density and textural triangles provide evidence on the plausibility of GIS methods based on geomorphology as do the pumping tests. The pumping tests, soil survey, and the GIS methods are each estimating K at different depths. The pumping tests are estimating K at the screen layer of the pumping test (~ +60m); the soil data are estimating K in the top ~1 to 7 m of soil and the GIS methods are estimating K for the entire saturated layer. The averaged difference of each method is compared to the soil data and the pumping tests.

While the Peuker Douglas Stream Order 1-7 had the lowest averaged difference of all the methods it also produced an unrealistic number of streams and catchments. The Peuker Douglas Stream Order 3-7 produced the next lowest average difference from Soil Survey K values and the method with the lowest average difference from the pumping tests.

Table 2.5. K (m/day) estimates at well locations for SSURGO Soil data, pumping tests and GIS methods.

OR Well Start No.	Soil Survey 2009	Pump tests	Manual Threshold (dropanalysis)	Length Area	Strahler Stream Order 7-12	Peuker Douglas Stream Order3-7	Approx. USGS 24K (low drainage density)	Peuker Douglas Stream Order 1-7
143834	0.78	0.24	2.74	0.61	3.05	1.22	276.45	1.22
131820	0.78	0.58	10.67	36.27	31.39	0.06	83.52	0.12
131817	0.78	0.09	6.40	2.13	1.22	0.30	320.34	0.30
128523	0.08	3.05E-05	0.15	0.15	0.15	0.03	54.86	0.03
127774	0.78	9.14E-05	1.22	31.39	0.91	0.30	21.03	0.43
83887	19.65	0.12	0.09	0.03	0.06	0.03	1.52	0.03
107079	0.78	0.24	2.13	14.33	1.83	0.61	25.30	0.61
67490	0.78	0.46	3.05	5.18	3.05	0.27	110.34	0.30
63838	0.78	1.83	0.09	0.12	1.22	0.09	64.31	0.09
54727	0.78	3.05E-05	1.83	2.74	1.83	2.13	8.53	2.13
44103	0.78	3.05E-05	7.62	1.52	7.92	0.30	19.81	0.30
33803	0.78	1.55	3.05	3.05	1.83	0.30	62.18	0.30
24125	0.78	9.14E-05	78.33	28.96	10.06	0.91	230.73	1.22
144876	0.78	1.58	2.13	2.44	2.13	0.61	50.90	0.61
Ave. Δ (Soil-Method)	na	1.60	-6.46	-7.13	-2.68	1.57	-92.91	1.53
Ave. Δ (pumping-method)	-1.60	na	-8.06	-8.73	-4.28	-0.03	-94.51	-0.07

The continuous K estimates from the 24K stream network exhibited the same overall pattern of high and low K values as the other stream delineation methods but were larger by one order of magnitude and did not exhibit the spatial variability of the other methods due to the larger catchments and averaging over catchments. Surprisingly, very large values of K(350+ m/day) were present in the 24K stream network which were not in the other methods as a result of increased W and small channel depth (d). The Peucker Douglas, stream order 1- 7, identified nonexistence stream networks and resulted in K estimates one order of magnitude less than the other methods (not including the USGS 24K method). This method led to very small downslope distances to streams, and larger valley depths and resulted in low K values. It has the largest spatial variability in K.

Bayesian kriging was conducted on the pumping locations to create interpolated grid estimates of K. While the interpolated values are reasonable when compared to the soil survey K estimates the spatial pattern of K along the stream beds was not identified. Additional pumping tests would have improved the interpolated surface but were not available. Low estimated K values from the pumping tests do follow the Oak Creek streambed and are shown as red symbols in fig. 2.4.

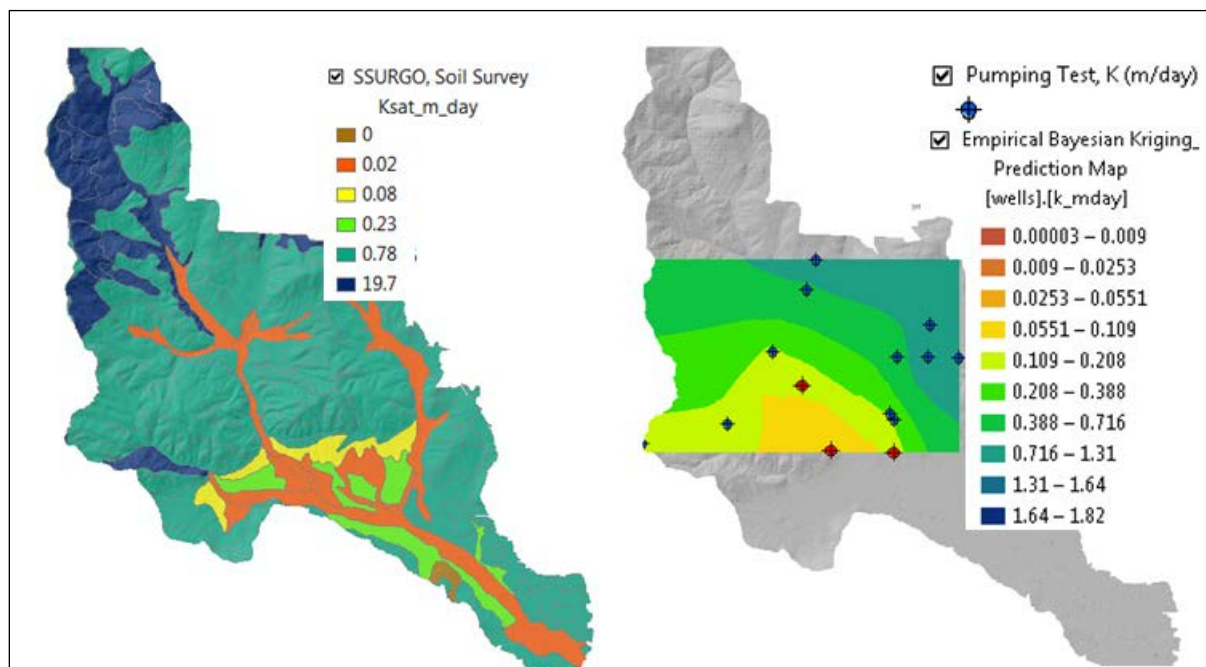


Figure 2.4. Published Krep (m/day) SSURGO soil data, interpolated K (m/day) estimates from pumping tests, and pumping locations. Red pumping symbols represent low K values, which are located by Oak Creek Stream and low K soil.

Figure 2.5 illustrates a single small catchment in Oak Creek which shows six stream generation methods with their estimated K values. The 24K method (e) is similar to the other methods but does not have any streams generated in this catchment and results in lower spatial variability of K values and larger K values. The Peuker Douglas stream order 1-7 (f) created nonexistent streams, which resulted in the highest spatial variability and K values smaller by one order of magnitude in comparison to methods a-d. Methods a-d produced similar K estimates. The differences in the K estimates are due to the location of drainage paths and corresponding overland flow distance to each stream and averaged catchment channel depth. The overall spatial pattern of K, abrupt edges between K values, is from the soil infiltration layer. Table 2.6 compares two locations of K estimates for each of the methods a-f shown in figure 2.5. K values in the top dark blue regions of the test catchment range from approximately 6 m/day to 271 m/day. K values at the stream entrance into the catchment on lower left side ranges from 0 – 1.20 m/day.

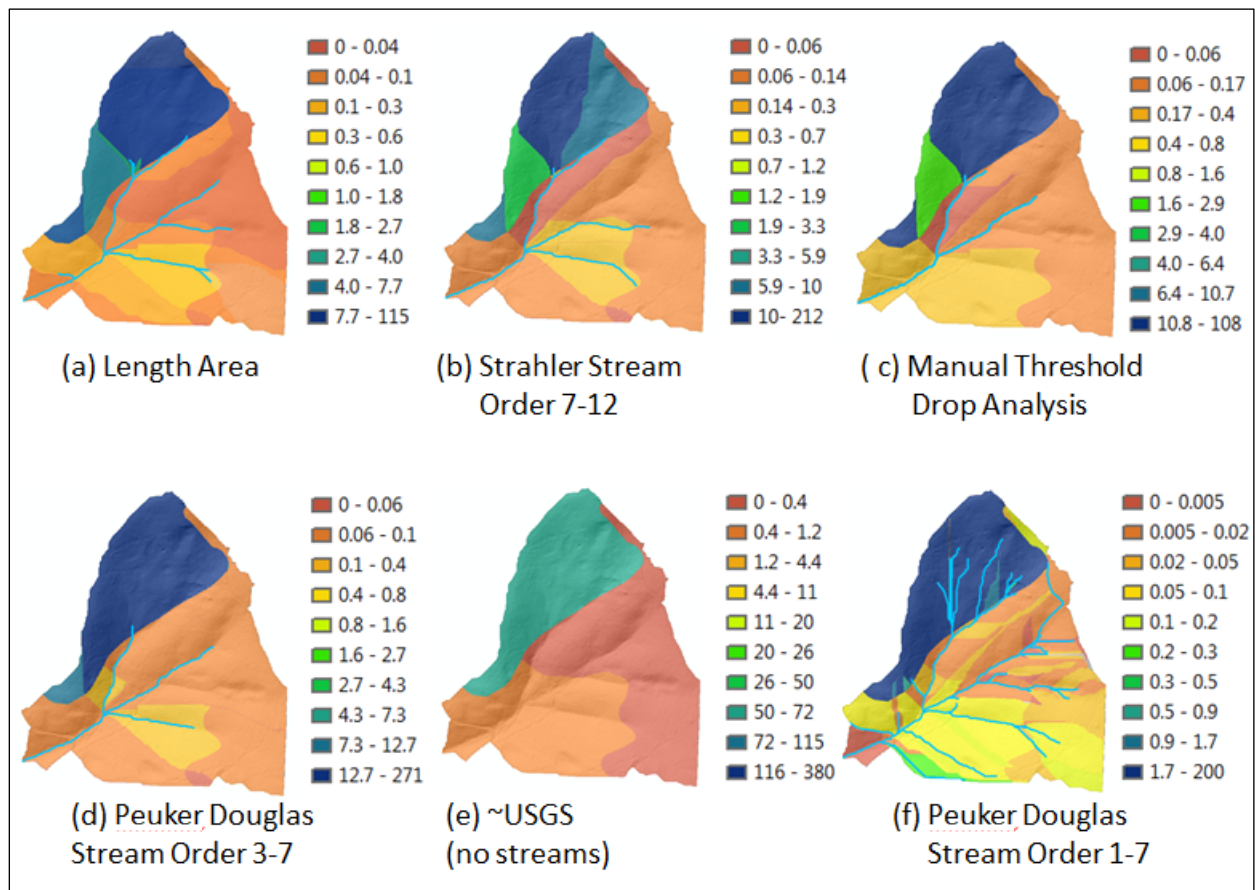


Figure 2.5. Single catchment with streams and K (m/day) from GIS different methods. Similar drainage density for all methods except ~USGS and Peuker Douglas 1-7. Thematically mapped with quartile, 10 classes (equal distribution of cells in each class).

Table 2.6. Comparison of K estimates for small test catchment shown in figure 2.5.

	Top of Catchment	Stream Entrance on Left
Method	K est. (m/day)	K est. (m/day)
A	7.5-115	0.04-0.10
B	5.9-212	0.06-0.14
C	10.8-108	0.40-0.80
D	12.7-271	0.06-0.10
E	50.0-72	0.40-1.20
F	1.7-200	0-0.0005

Discussion and Conclusions

This study demonstrated the effect of different stream generation methods on continuous estimates of aquifer hydraulic conductivity using a GIS approach. Independent sources have been used to verify the plausibility of the results ranging from well pumping tests to soil survey data. Pumping tests provide estimates at the screened interval with the aquifer and not the entire saturated layer and therefore are not directly comparable to the other methods. Similarly, K estimates from the soil survey data represent only the near-surface conditions in the aquifer. The pumping tests conductivity estimates are lower than the GIS estimates which are expected since hydraulic conductivity typically decreases as increased depths occur due to the sedimentation process occurring over large time periods.

The soil survey data provides K estimates for the surface soil and it is important to note about 57 percent of Benton County foothills and mountainous soil areas were compiled from aerial photography and interpretations for the soil surveys (USDA, NRCS, 2009) and not field sampled or tested. A large difference between the soil survey data and the GIS estimates occur in the northwestern part of Oak Creek watershed. Soil survey data indicate K is the largest in this region of the watershed and the GIS estimates do not reflect this. This is the region where weathered bedrock exists. One possible explanation is that the estimated infiltration percentages were incorrect (table 2.2).

In general the GIS K estimates were distributed similarly to those based on soil survey and related infiltration estimates. Clays and silty clays have small infiltration rates and typically correspond to lower K values, while silty loams and cobbly-loams have larger infiltration rates and correspond to higher K values. Infiltration rates are directly related to recharge estimates. The change of infiltration by one order of magnitude changes K by one order of magnitude. In all

GIS methods, the aquifer thickness was assumed to be constant, but sensitivity analyses show that uncertainties in aquifer thickness do not significantly affect K estimates (Lou et al., 2011). The most sensitive parameter for each algorithm is W, the downslope distance to the nearest stream. Each stream delineation algorithm generates slightly different streams and affects the overland flow distance to the nearest stream; increasing W and increasing K.

This study offers supporting evidence that basin-scale GIS estimates of aquifer hydraulic conductivity were similar for many proven stream delineation methods. In addition, a robust or morphology-based algorithm does not appear to be essential to obtain plausible estimates of K but accurate identification of the watershed stream density is important. A GIS technique proves to be efficient and effective especially when field data are limited and by the fact that hydraulic conductivity can vary within small regions by up to four orders of magnitude (Manning and Ingebritsen, 1999). This technique of estimating K through drainage patterns has been applied to the Oregon Cascades and High Plain Aquifer [Lou et al., 2011, 2001 and Lou and Pederson, 2012] and shown to provide plausible results. The methods in this study followed the methods described in Lou and Pederson (2012) with the exception they used a 37.2 m resolution DEM and this study used 1 meter DEM. Lou and Pederson (2012) also used a terrain morphology-based algorithm by Molloy and Stepinski (2007) for stream delineation and this study used six different methods with the morphology-based algorithm from Tarboton and Ames (2001). Lou and Pederson (2012) state Tarboton and Ames morphology-based delineation method seems to work well for small single basins, which Oak Creek watershed represents. This study is different in that it is a small watershed and used a high resolution LiDAR DEM. The LiDAR DEM proved to be an excellent source for delineating stream networks and accurately calculating downslope distance to streams and channel depths. Whether LiDAR DEM is better suited for estimating hydraulic conductivity than a 10 meter DEM for a small watershed still needs to be investigated but channel depths would be smoothed in a coarser DEM.

The method is sensitive to the estimate of recharge which in this study was estimated with infiltration (soil classification) and precipitation. In 1998, Woodard and others studied groundwater recharge for the Willamette Lowland aquifer system where the regional mean annual recharge was estimated about 42 percent of the mean annual precipitation. From Woodard's estimate, the mean recharge for the Oak Creek watershed is 0.58 m/yr and in the study it was estimated to be $0.29 - 1.22 \times 10^{-3}$ m/yr. The methodology was validated in a study area with silty clay loam and silty loam but needs to be validated in other soils

Drainage patterns are influenced by groundwater systems and this study's method implicitly takes into account topography, soil and climate from readily available data to estimate

plausible continuous hydraulic conductivity at a basin-wide scale. The method of stream delineation does not appear to affect results. By using the strengths of GIS with the best data available, we can increase the effectiveness of our estimates of K basin-wide.

Literature Cited

Conlon, T. D, Wozniak, K. C., Woodcock, D., Herrera, N. B., Fisher, B. J., Morgan, D. S., Lee, K. K, Hinkle, S. R., 2005. Ground-Water Hydrology of the Willamette Basin, Oregon. USGS, Scientific Report 2005-5168.

Domenico, P. A., Schwartz, F. W., 1990. Physical and Chemical Hydrogeology. Wiley & sons, New Jersey.

Goodchild, M. F., 1992. Geographical information science. International Journal of Geographical Information Systems, 6, 31-45.

Goodchild, M. F., Parks, B. O., Steyaert, L.T., Johnston, 1996. GIS and Environmental Modeling: Progress and Research Issues. John Wiley & Sons, New Jersey.

Gupta, N., Rudra, R.P., and Parkin, G. Analysis of spatial variability of hydraulic conductivity at field scales. Canadian Biosystems Engineering, 48, 1.55-1.62.

Gurnell, A.M., and Montgomery, D.R, 2000. Advances in Hydrologic Processes: Hydrological Applications of GIS. John Wiley & Sons, New York.

Fotheringham, A. S., and Rogerson, P. A., 1994. Spatial Analysis and GIS. Taylor & Francis, London.

Jha, M.K., Chowdhury, A., Chowdary, V.M., Peiffer, S. 2007. Groundwater management and development by integrated remote sensing and geographic information system: prospects and constraints. Water Resources Management, 21, 427-467.

Lagacherie, P., McBratney, A.B., Voltz, M., Digital Soil Mapping An Introductory Perspective. - Developments in Soil Science Series, Elsevier Publisher, Ch. 43.

Lee, K. K. and Risley, J.C., 2002. Estimates of Ground-Water Recharge, Base Flow and Stream-Reach Gains and Losses in the Willamette River Basin, Oregon. USGS, Portland, Oregon.

Luo, W. and Pederson, D. T., 2012. Hydraulic conductivity of the High Plains Aquifer re-evaluated using surface drainage patterns. Geophysical Research Letters, 39, 1-6.

Luo, W., Grudzinski, B. P., Pederson, D., 2010. Estimating hydraulic conductivity from drainage patterns: a case study in the Oregon Cascades. Geology, 38, 335–338.

Luo, W., Grudzinski, B. P., Pederson, D., 2011. Estimating hydraulic conductivity for the Martian subsurface based on drainage patterns: a case study in the Mare Tyrrhenum Quadrangle, Geomorphology 125, 414–420.

- Luo, W., Stepinski, T.F., 2007. Topographically derived maps of valley networks and drainage density in the Mare Tyrrhenum quadrangle on Mars. *Geophysical Research Letters* 33.
- Luo, W., Stepinski, T.F., 2008. Identification of geologic contrasts from landscape dissection pattern: an application to the Cascade Range, Oregon, USA. *Geomorphology*, 99, 90-98.
- Maidment, D. R., 1993. GIS and hydrologic modeling. In: *Environmental Modeling with GIS*. Goodchild, M. F., Parks, B. O., Steyaert, L. T. (Eds.). Oxford Press Univ. Press, NY, 147-167.
- Manning, C. E., and Ingebritsen, S. E., 1999, Permeability of the continental crust: constraints from heat flow models and metamorphic systems. *Reviews in Geophysics*, 37, 127-150.
- McDonnell, R. A., 1996. Including the spatial dimension: using geographical information systems in hydrology. *Progress in Physical Geography*, 20, 159-177.
- McElwee, C. D. (1980), Theis Parameter Evaluation from Pumping Tests by Sensitivity Analysis. *Ground Water*, 18, 56–60.
- Miles, Evans (2011). A GIS Study of Benton County, Oregon, Groundwater: Spatial Distributions of Selected Hydrogeologic Parameters, Oregon State University.
- Montgomery, D.R., Dietrich, W.E., 1989. Source areas, drainage density, and channel initiation. *Water Resources Research*, 25, 1907–1918.
- Montgomery, D.R., Dietrich, W.E., 1992. Channel initiation and the problem of landscape scale. *Science* 255 (5046), 826–829.
- Nash, J., Sutcliffe, J., 1970. River flow forecasting through conceptual models. Part I – a Discussion of Principles. *Journal of Hydrology* 10: 282-290.
- Neuman, S., 1990. Universal scaling of hydraulic conductivities and dispersivities in geologic media. *Water Resources Research* 26, 1749–1758.
- Neuman, S., 1994. Generalized scaling of permeabilities: validation and effect of support scale. *Geophysical Research Letters*, 21, 349–352.
- Peucker, T.K., Douglas, D.H., 1975. Detection of surface-specific points by local parallel processing of discrete terrain elevation data. *Computer Graphics and Image Processing*, 4, 375–387.
- Phillips, O.M., 2003. Groundwater flow patterns in extensive shallow aquifers with gentle relief: Theory and application to the Galena/Locust Grove region of eastern Maryland. *Water Resources Research*, 39, 1149-1163.
- Refsgaars, J.C., Hojberg, A.L., Moller, I., Hansen, M., Sondergaard, V., 2010. Groundwater modeling in integrated water resources management – visions for 2020. *Groundwater*, 48, 633-648.
- Rigon, Riccardo; Rodriguez-Iturbe, Ignacio; Maritan, Amos; Giacometti, Achille; Tarboton, David; and Rinaldo, Andrea, 1996. On Hack's Law. *Water Resources Research*, 32. 3367-3374.

Rodriguez-Iturbe, I., Rinaldo, A., 1997. *Fractal River Basins: Chance and Self-Organization*. Cambridge Univ. Press, New York.

Sánchez-Vila, X. Girardi, J. P., Carrera, J., 1995. A Synthesis of Approaches to Upscaling of Hydraulic Conductivities. *Water Resources Research*, 31, 867-882.

Surfleet, Christopher, 2008. PhD. Dissertation: Uncertainty in Forest Road Hydrologic Modeling and Catchment Scale Assessment of Forest Road Sediment Yield. Oregon State University, Department of Forestry.

Tarboton, D.G., 1997. A new method for the determination of flow directions and upslope areas in grid digital elevation models. *Water Resources Research*, 33, 309-319.

Tarboton, D.G., Ames, D.P., 2001. Advances in the mapping of flow networks from digital elevation data. *World Water and Environmental Resources Congress*. ASCE, Orlando, Florida.

Tucker, G.E., Catani, F., Rinaldo, A., Bras, R.L., 2001. Statistical analysis of drainage density from digital terrain data. *Geomorphology*, 36, 187–202.

USDA, NRCS, Soil Survey of Benton County, Oregon. 2009.

3. Equivalent Basin-Scale Hydraulic Conductivity: A GIS Approach

Abstract

Because of the disparity between the scales at which measurements are taken for traditional conductivity estimates and those required for hydrologic modeling, conductivity point data are typically upscaled to the meter-to-kilometer scale and then referred to as equivalent conductivities. The usage of the term *equivalent* reflects the fact that hydraulic conductivity is not an additive variable. Even though upscaling has been studied intensively, most work has focused on synthetic data sets, or otherwise idealized conditions (e.g., uniform layering, infinite spatial extents, log normal distribution) with known parameters, etc. Application of these techniques to real aquifer systems has been more limited. In particular, little work has been done on evaluating upscaling techniques for large natural watersheds, which are irregular in shape, finite in extent, and heterogeneous. The use of upscaling methods to estimate the equivalent hydraulic conductivity of a natural watershed has not been extensively studied. In particular, it is not well understood how to incorporate the geomorphology of the watershed (stream density, drainage paths, slope, etc.) into upscaling techniques. The objective of this study was to develop and test a new method for computing basin scale equivalent hydraulic conductivities (*Kequiv*) for use in hydrologic modeling and to explore the relationships of catchment and drainage paths equivalent conductivities to a watershed's equivalent conductivity using GIS.

Introduction

Estimating the hydraulic conductivity of earth materials is important for many water resource modeling efforts, including predicting the transport of pollutants in ground water, computing surface runoff for flood control, and computing water budgets. There is a disparity between the scales at which measurements are taken and those required for hydrologic modeling. Typically hydraulic conductivity data are obtained using field or laboratory measurements at the centimeter-to-meter scale and are upscaled to the meter-to-kilometer scale and then referred to as equivalent, upscaled, effective or block conductivities. The usage of the terms *equivalent*, *block*, *effective* or *upscaled*, rather than e.g., *average*, reflects the fact that hydraulic conductivity is not an additive variable – it is not possible to calculate an equivalent conductivity for a heterogeneous block by simply averaging point measurements. In addition, there are virtually no existing data sets that provide enough information to extensively validate existing upscaling approaches.

Upscaling can be conducted using either *local* or *nonlocal* techniques. Local techniques consider the block conductivity to be a property of the cell conductivity within the block, and are typically used in one-dimensional flow models. Nonlocal upscaling techniques consider block conductivities to depend on flow conditions within the block, which are determined, in part, by boundary conditions, and are typically used in two-dimensional flow modeling. In all methods, the objective of upscaling is to estimate conductivity values that reproduce the overall system behavior at the field scale.

Hydraulic conductivity describes the energy loss that occurs as water flows through a permeable medium, such as soil. It is a function of the properties of the porous medium and the fluid and is described by Darcy's Law. Although Darcy's Law is typically written assuming a homogeneous and isotropic porous medium, all geologic materials are heterogeneous and anisotropic. Heterogeneity and anisotropy are caused by the interaction of the geologic and geomorphic processes acting over very long times that formed the aquifer (e.g., sedimentation/deposition, erosion and tectonic processes). The result is geologic complexity - a complex arrangement of highly variable geologic materials. As a result of this complexity, hydraulic conductivity can vary over several orders of magnitude over both short and long horizontal and vertical distances.

Upscaling methods include: 1) averaging techniques, such as, arithmetic, geometric, harmonic means; 2) methods based on stochastic field theory (Matheron, 1967); and 3) regularization techniques (Norman, 1992; and Wen and Gomez-Hernandez, 1996). In these methods, flow is usually assumed to be either parallel or perpendicular to layering. From electric conductance analogy the equivalent hydraulic conductivity for a group of cells arranged serially is equal to their harmonic mean, and cells arranged in parallel is equal to the arithmetic mean.

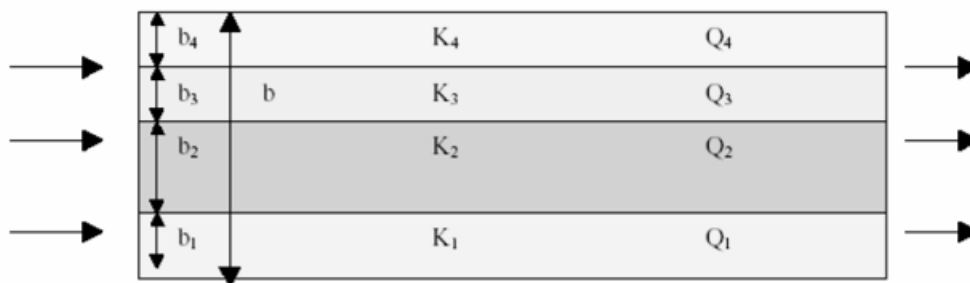


Figure 3.1. Flow parallel to layering: the equivalent conductivity is the weighted arithmetic mean of the individual layer values.

Equivalent hydraulic conductivity for flow parallel to layers is often calculated as a weighted arithmetic mean (K_A) (Oosterbaan and Nijland, 1994).

$$K_A = \frac{\sum K_i b_i}{\sum b_i} \quad (1)$$

For flow normal to geologic layering, the law of conservation of mass dictates discharge through each layer must be the same.

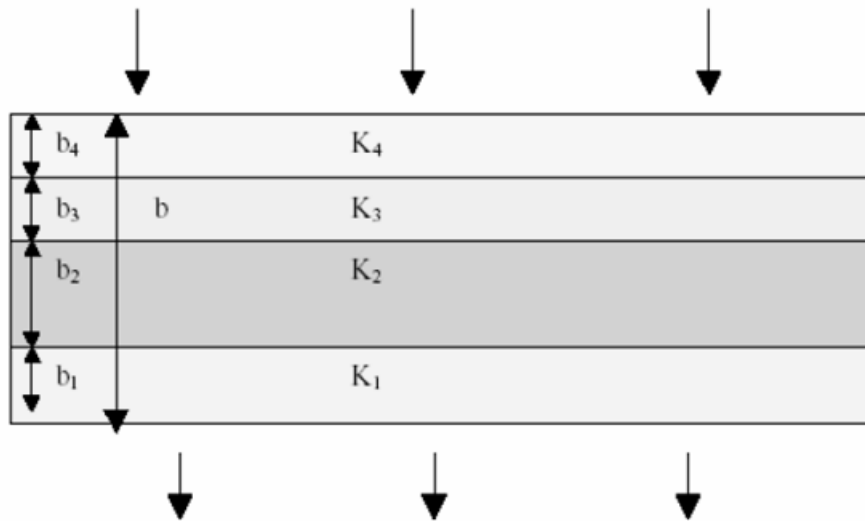


Figure 3.2. Flow perpendicular to layering: the equivalent K (L/T) is the weighted harmonic mean of the individual layer values.

The equivalent hydraulic conductivity is calculated as a weighted harmonic mean (K_H) for flow perpendicular to the geologic layering.

$$K_H = \frac{\sum b_i}{\sum \left(\frac{b_i}{K_i}\right)} \quad (2)$$

Many authors have demonstrated that equivalent conductivities of heterogeneous layers lie between the arithmetic and harmonic means of the cells for horizontal flow (Cardwell and Parsons 1945; Matheron, 1967; and Dagan, 1993).

$$K_A \leq K_{equiv} \leq K_H \quad (3)$$

Where K_{equiv} = the equivalent conductivity, K_H = harmonic mean and K_A = arithmetic mean. For 1D flow, Hashin and Shtrikman (1962) demonstrated the equivalent hydraulic conductivity in a macroscopically homogenous and isotropic material to be bounded by either the harmonic or arithmetic mean block values. Matheron (1967) found equivalent conductivity to be equal to the geometric mean for infinite blocks with heterogeneity and isotropic spatial correlation and frequency distribution of their reciprocals (assuming that conductivity follows a lognormal distribution). Durlofsky (1992) studied uncorrelated, correlated, statistically isotropic and anisotropic, and sand-shale binary distributions using simple average methods including: arithmetic, geometric, harmonic, arithmetic-harmonic and harmonic-arithmetic and concluded there are no simple averaging techniques that are valid for all heterogeneous materials.

Gomez-Hernandez and Wen (1994) determined, in 2D, the geometric mean provides reliable estimates of block conductivity as long as strong anisotropy is not present (Wen and Gomez-Hernandez, 1996). The geometric mean

$$K_G = \sqrt[n]{(K_1 K_2 \dots K_n)} \quad (4)$$

where n is the total number of observations. In terms of $\log K$ in equation (4) becomes

$$\text{Log } K = (\log K_1 + \text{Log } K_2 + \dots + \log K_n) / n \quad (5)$$

From equation (5), it can be seen K_G is the arithmetic mean of the $\log K$ -values. This corresponds to the mean value of log-normal distribution.

Journel et al. (1986) used power averaging to estimate equivalent block conductivities, with the power exponent (p) ranging from -1 to 1; when $p = 0$ it represents the geometric mean, $p = -1$, the harmonic mean and when $p = 1$ it represents the arithmetic mean. Several authors have successfully applied Journel's power averaging in numerical simulations (Gomez-Hernandez and Gorelick (1989), Bachu and Cuthiell (1990) and Desbarats (1992)).

Other upscaling methods are based on stochastic field theory. For example, Vidstrand (2001) found field scale hydraulic conductivity values to be a subset of the entire, small-scale data set and hydraulic conductivity values should statistically behave in the same manner when scaled up. Matheron (1967) showed that the equivalent hydraulic conductivity for a flow domain is

$$\underline{K_{equiv}} = K_G * e^{[(\frac{1}{2} - \frac{1}{m})\sigma^2 \ln]} \quad (6)$$

where K_G is the geometric mean, m is the dimensionality (i.e. $m=1$ for 1D flow etc.), and σ^2_{\ln} is the variance in the natural logarithm of the hydraulic conductivity, with the assumption of isotropic, log-normal, stochastic field of values with large flow volume.

It is well established that the arithmetic and harmonic means of point K values represent the equivalent horizontal and vertical conductivities, respectively, for an infinite horizontal medium with layers of uniform thickness (Zang, et al., 2007). For heterogeneous lithology, harmonic and arithmetic means constitute the upper and lower bounds of the equivalent conductivities (Renard and de Marsily, 1997). For 2D log-normally distributed conductivity, the geometric mean has been found to represent the equivalent conductivity of the point K values (Matheron, 1967).

Even though upscaling has been studied intensively (Tran, 1995; Yamada, 1995; Wen, 1996; Wen and Gomez-Hernandez, 1996), most work has focused on synthetic data sets, or otherwise idealized conditions (e.g., uniform layering, infinite spatial extents, log normal distribution) with known parameters, etc. Application of these techniques to real aquifer systems has been more limited. In particular, little work has been done on evaluating upscaling techniques for large natural watersheds, which are irregular in shape, finite in extent, and heterogeneous. The use of upscaling methods to estimate the equivalent hydraulic conductivity of a natural watershed has not been extensively studied. In particular, it is not well understood how to incorporate the geomorphology of the watershed (stream density, drainage paths, slope, etc.) into upscaling techniques. The objective of this study was to develop and test a new method for computing basin scale equivalent hydraulic conductivities (*Kequiv*) for use in hydrologic modeling and to explore the relationships of catchment and drainage paths equivalent conductivities to a watershed's equivalent conductivity using Geographic Information Systems (GIS).

Site Description

The study was performed on the Oak Creek watershed, a catchment in the Upper Willamette 8-digit Hydrologic Unit Code (17090003) subbasin, located in Benton County, OR. The Upper Willamette watershed is equivalent of the other Willamette basin watersheds (Yamhill, Tualatin, Middle Willamette, etc.) with respect to soils, topography, precipitation and climate. Oak Creek watershed is located in the McDonald/Dunn Research Forest managed by

the College of Forestry, Oregon State University. The watershed area is ~ 3360 hectares; elevations range from 60 to more than 585 meters. The average annual precipitation for 1971-2000 was 137 cm/yr with a range of 107-188 cm/yr. Precipitation in the watershed is predominantly rain (~ 95 %). The underlying bedrock, the Siletz River Volcanics, is a basalt formation. The most common surface soil texture is silty clay loam, although some silty loam is also present. The forest trees are predominantly Douglas-fir with minor components of other conifers, hardwood species, and grassy meadows. There is a meteorological station near the outlet of the study watershed where continuous observations of air temperature, relative humidity, solar radiation, wind speed, and precipitation have been made since 2003. In addition, there are three rain gauges located in the watershed.

Methods

Horizontal hydraulic conductivity for the entire saturated thickness of the aquifer was estimated across Oak Creek watershed using geomorphology and GIS (Arras and Istok, 2014, manuscript in progress) based on methods developed by Lou et al., 2008, 2010, and 2011. This approach assumes 1) the aquifer is effectively drained (recharge equals discharge) and that surface morphology is in steady-state dynamic equilibrium through the interplay of surface water, groundwater and topography (valley network formation has ceased and drainage density is stable) and 2) groundwater flow is described by Darcy's Law, and the DuPuit-Forchheimer assumptions (that the aquifer is unconfined and flow is primarily horizontal) apply (Lou et al, 2011). With these assumptions, hydraulic conductivity, K , was estimated for every cell in the watershed

$$K = \frac{4W^2R}{[H^2 - (H - d)^2]} \quad (7)$$

where K is hydraulic conductivity [L/T]; W is length of effective groundwater drainage [L]; D is drainage density [1/L]; R is recharge rate [L/T]; d is valley depth [L]; and H is aquifer thickness [L].

A USGS 10 meter resolution digital elevation model (DEM) with a vertical accuracy of 3 meters was used to delineate drainage paths based on a contributing area of 154 m² (0.038 acres), which resulted in 394 catchments within the Oak Creek watershed. Aquifer thickness, H , was assumed constant ($H = 98.4$ m) in this study, based on estimates from USGS Scientific Investigations Report 2005-5168. The valley depth, d , was calculated with a Black Top Hat (BTH) transformation technique that utilized a moving neighborhood radius of 4 cells, to extract

channel depths, which were averaged over each catchment (Lou and Pederson, 2012). Spatially varying recharge, R , was estimated from precipitation and soil data, by assuming recharge equals the precipitation times the soil infiltration percentage.

The 30-year (1971–2000) gridded mean annual precipitation data was obtained from Oregon State University, PRISM Climate Group. Soil Survey Geographic Database (SSURGO) was obtained from USDA-NRCS, which was assigned an infiltration percentage based on soil texture classification (Table 3.1) (Lou and Pederson, 2012). This method of estimating recharge implicitly takes into consideration the spatial variability due to climate, soil, vegetation, and topography (Lou and Pederson, 2012). Parameters: W , R , and d were all individually averaged by each catchment.

Table 3.1. Estimated infiltration percentage by soil texture classification (Lou and Pederson, 2012).

Soil Texture Classification	Estimated Infiltration Percentage
Unweathered Bedrock	0.1
Clay	0.2
Weathered Bedrock	1
Silty Clay	2
Gravelly Clay	3
Paragravelly Clay	3
Loam	5
Silty clay loam	5.5
Silty Loam	8.5
Very Cobbly Loam	15.5
Very Paragravelly Loam	15.5
Decomposed Plant Material	18

The boundaries of 394 catchments were compiled using standard techniques developed by Maidment with the D8 overland flow technique (Arras and Istok, 2014, manuscript in progress). Figure 3.3 represents the continuous hydraulic conductivities at the measurement cell scale for 394 catchments. For evaluation of equivalent conductivity in this study, the 394 catchments were merged together to form larger catchment areas based on surface drainage (merged adjoint catchments) and formed 54 catchments. The final 54 catchments of the watershed are similar to the digital 1:24,000 National Hydrology Dataset (NHD) and were used as the geographic boundaries for calculating catchment equivalent hydraulic conductivities.

Catchment numbering starts with zero in the upper reaches of the watershed and increases in numbering until the outlet is reached.

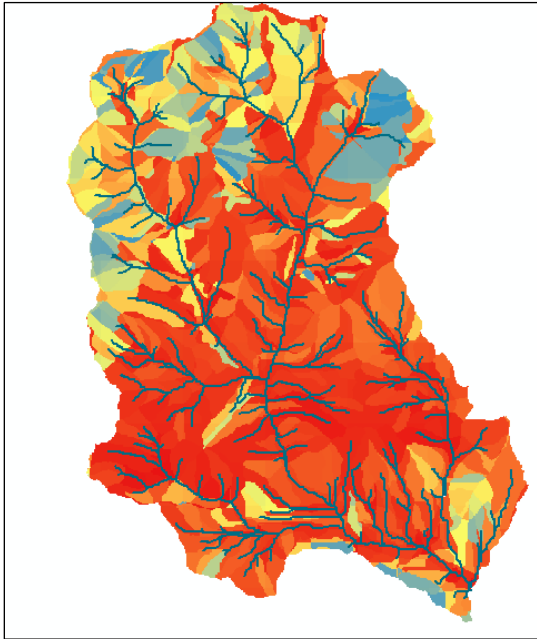


Figure 3.3. Continuous K (m/day) estimates from Geomorphologic-GIS method using a USGS 10 meter DEM. K ranges from 0.01-18 m/day. Dark blue represents the largest values of K , orange are mid values and yellow, lowest values, respectively. Drainage paths are overlaid in blue.

A new GIS version of the harmonic mean was used to determine an equivalent conductivity for flow along any horizontal flow path. In this approach the $Kequiv$ for the flow path is the harmonic mean, weighted by the portions of the flow path within each conductivity zone. $Kequiv$ can be calculated using two similar but slightly different approaches. When calculating $Kequiv$ along linear drainage paths, such as stream channels, flow starts upstream and moves downstream to lower stream reaches, and the new equivalent hydraulic conductivity is

$$Kequiv = \frac{\sum L_T}{\sum (L_{ki} / k_i)} \quad (8)$$

Where $Kequiv$ is the equivalent hydraulic conductivity determined from the harmonic mean, L_T is the horizontal length of the entire drainage path being evaluated, and L_{ki} is the horizontal length within each conductivity zone i for each conductivity value and K_i is the respective conductivity value for zone i . To calculate the harmonic mean for hydrologic areas which are not linear features, such as catchments or watersheds, raster analysis is used in conjunction with overland flow theory. Overland flow moves in one of the eight cardinal directions as described

by Maidment (2002), determined by steepest descent (slope) method. Lengths are determined by moving from the center of one cell to the center of the neighboring cell, along the flow direction. Horizontal lengths are the raster cell size and the diagonal lengths are the distance along the hypotenuse from the center of a cell to the center of the neighboring cell along the overland flow path. Because the total linear distance is in the numerator and the linear distance for each zone is in the denominator it can be removed from the expression for an approximation. Thus, only the total number of cells in the equivalent area and the total numbers of cells per conductivity are required.

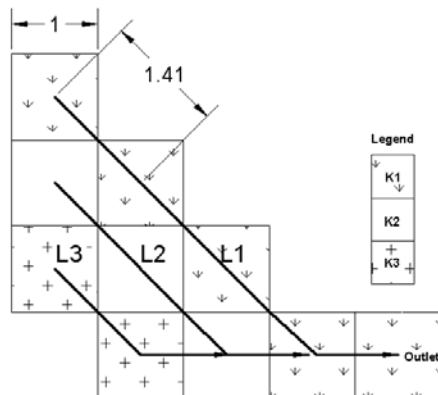


Figure 3.4. Illustration of raster flow directions and corresponding lengths used to calculate equivalent conductivity. The cell size is 1; horizontal length is 1 unit and length along the diagonal is $\sqrt{2}$ units.

Figure 3.4 shows lengths of the three overland flow paths and the *Kequiv* for the catchment's outlet point. Calculations are provided below:

$$\sum L_1 = 3(\sqrt{2}) + 1(1) = 5.23 \text{ ft; overland flow path L1}$$

$$\sum L_2 = 2(\sqrt{2}) + 1(1) = 3.82 \text{ ft; overland flow path L2}$$

$$\sum L_3 = 1(\sqrt{2}) + 1(1) = 2.41 \text{ ft; overland flow path L3}$$

$$\sum L_{123} = 11.46 \text{ ft; total overland length of catchment: L1, L2, and L3}$$

$$L_1/k_i = 3(\sqrt{2}) / (K1) + 1(1) / (K1) = 5.23 / K1$$

$$L_2/k_i = 2(\sqrt{2}) / (K2) + 1(1) / (K2) = 3.82 / K2$$

$$L_3/k_i = 1(\sqrt{2}) / (K3) + 1(1) / (K3) = 2.41 / K3$$

It is assumed the cell value of K takes the value of the “from cell” when moving in the direction of a cell with a different K value and the cell is square. $Kequiv$ for the sample catchment shown in figure 3.4 is

$$\begin{aligned} Kequiv &= \sum L_{123} / \sum L_i / k_i \\ &= 11.46 / (5.23/K_1 + 3.82/K_2 + 2.41/K_3) \end{aligned}$$

$Kequiv$ can be approximated as

$$\sum(\text{no. grid cells in area}) / \sum (K_i \text{ no. cells} / K_i) \quad (9)$$

Following the example in figure 3.4:

$$\sum \text{No. of Catchment Cells} = 10 \text{ cells}$$

$$\sum \text{No. of } k_1 \text{ cells} / k_1 = 5 / K_1$$

$$\sum \text{No. of } k_2 \text{ cells} / k_2 = 3 / K_2$$

$$\sum \text{No. of } k_3 \text{ cells} / k_3 = 2 / K_3$$

$$\begin{aligned} \text{Catchment } Kequiv &= \sum \text{Catchment Cells} / \sum \text{No. of cells } K_i / K_i \\ &= 10 / (5 / K_1 + 3 / K_2 + 2 / K_3) \end{aligned}$$

$Kequiv$ is essentially the standard harmonic mean shown in eqn. 2 but instead of using discrete data points, continuous (raster) data are used. The cells of the raster represent point data in the analysis. The method to calculate $Kequiv$ can use either raster or vector data. The study calculated $Kequiv$ for Oak Creek watershed and for individual catchments using three different approaches:

1. $Kequiv_a$; which used all the cells in the block area, such as catchment or watershed

$$\sum(\text{no. cells in block area}) / \sum (K_i \text{ no. cells in area} / K_i)$$

2. $Kequiv_{dp}$; used only the cells in the major and minor drainage paths (streams)

$$\sum(\text{no. cells in all drainage paths}) / \sum (K_i \text{ no. cells in all drainage paths} / K_i)$$

3. $Kequiv_{mdp}$; used only the cells in the watershed's major drainage paths

$$\sum(\text{no. cells in major drainage paths}) / \sum (K_i \text{ no. cells in major drainage paths} / K_i)$$

The above *Kequiv* versions (1-3) use all the cells in the geographic feature, whether the area is a catchment, watershed or stream drainage path. As an example, the watershed $Kequiv_{mdp}$, uses only the cells in the major stream drainage paths within the watershed (figure 3.5). Catchment $Kequiv_a$ values used the cells bounded by the catchment and the resulting *Kequiv* was represented at the catchment's drainage outlet point (figure 3.5). A catchment's drainage outlet point is the point in the catchment where all surface drainage exits the catchment. Oak Creek stream was selected as the major drainage path to investigate because it is the major river reach in the watershed, provides the greatest range in topographic relief, and represents the longest drainage path in the watershed.

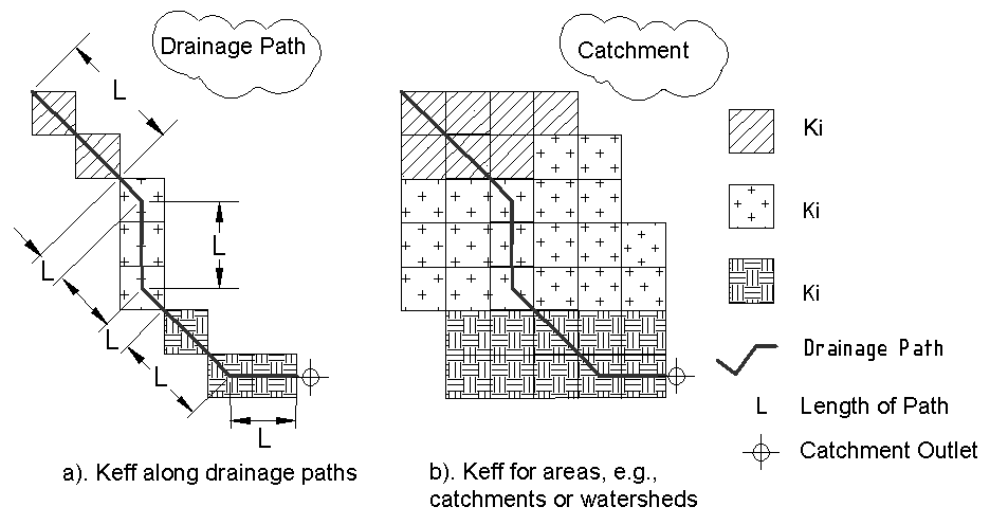


Figure 3.5. New *Kequiv* (L/T) for drainage paths and areas.

K_A , weighted arithmetic mean (1D flow), and K_G , geometric mean (2D flow), were also computed for comparison using cells as individual point conductivity values. K_A used eqn. (1) and layer thickness (b_i) was the number of cells in the feature by using the same analogy that was used for eqn. (9). The geometric mean used eqn. (5) and n was the total number of cells in the feature under investigation.

Results

The Oak Creek watershed contained 304,299 cells, each with an estimated hydraulic conductivity obtained through geomorphology and GIS that ranged from 0.01 to 18.01 m/day. Because hydraulic conductivity is not an additive property, upscaling was conducted to estimate equivalent conductivities for the catchments and for the entire watershed. Table 3.2 depicts

$Kequiv_a$, K_A , K_G , $Kequiv_{dp}$, difference between K_A - $Kequiv_a$, and difference between $Kequiv_a$ - $Kequiv_{dp}$ for the individual catchments. It is important to note, while K_G has been provided it is typically associated with 2D flow. The results show that when $Kequiv$ is calculated for an area with the arithmetic mean (K_A) it is typically greater than when calculated with the geometric mean (K_G), and typically greater than when calculated with the harmonic mean or in this study $Kequiv_a$ (table 3.2, and fig.3.6 and 3.7. It can be seen by comparing eqns. (1) and (2) that the equivalent conductivity determined from the arithmetic mean is determined predominantly by cell data with the highest conductivity values, whereas the harmonic mean is predominantly determined by cell data with the lowest conductivity values.

Table 3.2. Equivalent hydraulic conductivities (m/day) and differences.

Cat (1)	$Kequiv_a$ (2) m/day	K_A (3) m/day	K_G (4) m/day	$Kequiv_{dp}$ (5) m/day	Diff(K_A - $Kequiv_a$) (6) m/day	Diff($Kequiv_a$ - $Kequiv_{dp}$) (7) m/day
0	0.49	1.31	0.90	1.54	0.82	-1.05
1	1.27	2.60	1.95	1.12	1.33	0.15
2	1.02	2.18	1.52	1.10	1.17	-0.08
3	1.03	3.00	1.84	0.47	1.97	0.56
4	0.33	1.82	0.86	0.65	1.49	-0.32
5	0.66	6.01	2.76	0.27	5.36	0.39
6	0.30	1.10	0.45	0.29	0.80	0.01
7	0.68	2.47	1.38	0.23	1.79	0.45
8	1.25	3.46	2.20	1.24	2.21	0.01
9	1.42	1.65	1.53	1.36	0.23	0.06
10	0.63	1.85	1.16	1.01	1.22	-0.38
11	0.64	0.73	0.51	0.31	0.09	0.33
12	0.30	1.65	0.61	0.17	1.35	0.13
13	0.35	0.86	0.49	0.28	0.51	0.07
14	0.11	0.29	0.16	0.09	0.18	0.02
15	0.35	0.76	0.47	0.25	0.41	0.10
16	0.26	1.10	0.66	0.23	0.84	0.03
17	0.21	0.54	0.38	0.15	0.33	0.06
18	0.28	0.47	0.34	0.23	0.19	0.05
19	0.15	0.43	2.76	0.24	0.28	-0.09
20	0.45	2.37	0.61	0.51	1.92	-0.06
21	0.15	0.26	0.21	0.07	0.11	0.08
22	0.25	0.78	0.42	0.09	0.52	0.16
23	0.07	0.25	0.14	0.04	0.18	0.03
24	0.29	0.78	0.48	0.19	0.48	0.10
25	0.28	0.55	0.36	0.20	0.27	0.08
26	0.31	0.46	0.48	0.16	0.15	0.15
27	0.44	0.67	0.47	0.13	0.23	0.31

Cont. Table 3.2 Equivalent hydraulic conductivities (m/day) and differences.

Cat (1)	Kequiv _a (2) m/day	K _A (3) m/day	K _G (4) m/day	Kequiv _{dp} (5) m/day	Diff(K _A -Kequiv _a) (6) m/day	Diff(Kequiv _a -Kequiv _{dp}) (7) m/day
28	0.24	0.94	0.44	0.14	0.70	0.10
29	0.25	0.35	0.31	0.16	0.10	0.09
30	0.15	0.15	0.15	0.14	0.00	0.01
31	0.25	0.32	2.76	0.19	0.07	0.06
32	0.15	0.17	0.16	0.13	0.02	0.02
33	0.42	0.88	0.66	0.41	0.45	0.01
34	0.17	0.30	0.20	0.18	0.13	-0.01
35	0.15	0.39	0.22	0.11	0.24	0.04
36	0.12	0.16	0.14	0.09	0.05	0.03
37	0.07	0.15	0.31	0.06	0.08	0.01
38	0.29	0.37	0.33	0.16	0.08	0.13
39	0.06	0.12	2.76	0.04	0.06	0.02
40	0.79	1.25	1.01	0.37	0.46	0.42
41	0.07	0.25	0.13	0.04	0.18	0.03
42	0.10	0.35	0.18	0.08	0.24	0.02
43	0.16	0.25	0.20	0.15	0.08	0.01
44	0.61	1.21	0.84	0.31	0.60	0.30
45	0.19	0.26	0.22	0.15	0.07	0.04
46	0.32	0.44	0.37	0.22	0.12	0.10
47	0.29	0.88	0.54	0.12	0.59	0.17
48	0.30	0.40	0.35	0.21	0.10	0.09
49	0.24	1.65	0.61	0.11	1.41	0.13
50	0.16	0.27	0.21	0.13	0.11	0.03
51	0.30	1.36	0.49	0.14	1.06	0.16
52	0.23	1.11	0.14	0.12	0.89	0.11
53	0.43	1.72	0.93	0.09	1.29	0.34
Ave. diff =					0.66	0.07

- (1) Catchment number - numbering starts in upper reaches and progresses towards outlet
(2) Kequiv_a - new harmonic mean method by using catchment cell data to estimate catchment Kequiv
(3) K_A – traditional arithmetic mean method but with catchment cell data to estimate catchment Kequiv
(4) K_G – traditional geometric mean method but with catchment cell data to estimate catchment Kequiv
(5) Kequiv_{dp} -new harmonic mean method by using stream path cell data to estimate catchment Kequiv

The Kequiv_{dp} and Kequiv_a are the study's harmonic methods to estimate equivalent conductivity for flow parallel to heterogeneous layering and K_A is the standard arithmetic method for homogeneous layering. Kequiv_{dp} uses a linear approach using only the drainage paths; cell

data are converted to vector to represent the linear features of drainage paths and $Kequiv_a$ uses a raster approach for hydrologic areas. The average difference between the catchment equivalent conductivities for the 54 catchments using the area method of $Kequiv_a$ and the linear feature method of $Kequiv_{dp}$ is 0.07 m/day. Overall, the two harmonic methods, $Kequiv_a$ and $Kequiv_{dp}$ produce surprisingly similar catchment equivalent conductivities throughout the watershed. The largest difference between $Kequiv_a$ and $Kequiv_{dp}$ was 1.05 m/day, which occurred in the head waters of the watershed at catchment 0. This was the result of larger cell conductivity values in the drainage path than in the catchment. The smallest difference between $Kequiv_a$ and $Kequiv_{dp}$ was 0.01 m/day (absolute value) and this occurred in 7 catchments. Similar catchment values of $Kequiv_a$ and $Kequiv_{dp}$ meant the conductivity values in the drainage path cells were representative of cell values in the corresponding catchment.

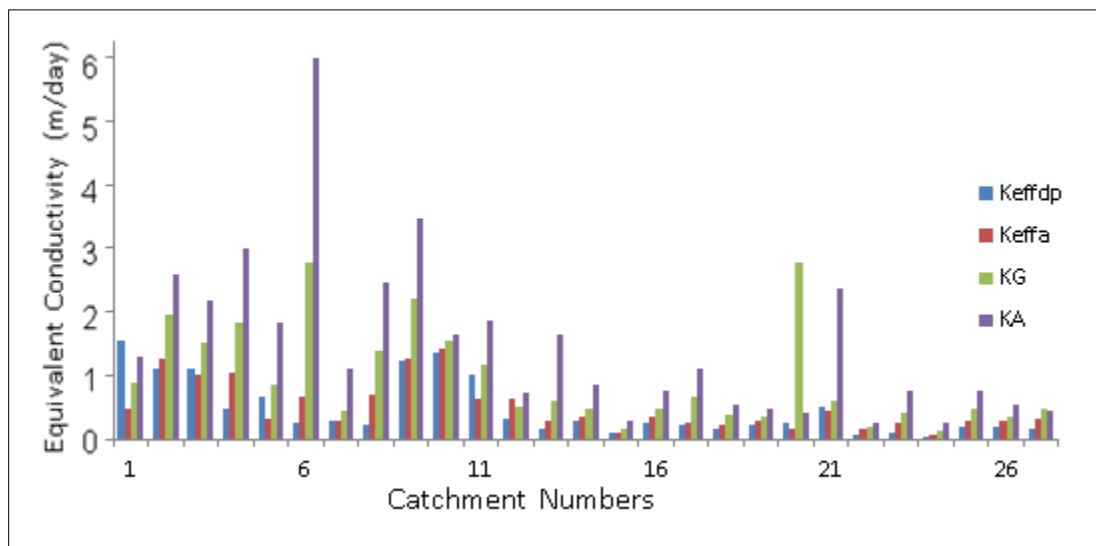


Figure 3.6. Catchment equivalent conductivity (m/day) estimated using the different approaches: $Kequiv_{dp}$, $Kequiv_a$, K_G and K_A for each of the 54 catchments. Catchment numbers 1-26 represent the upper catchments of the watershed.

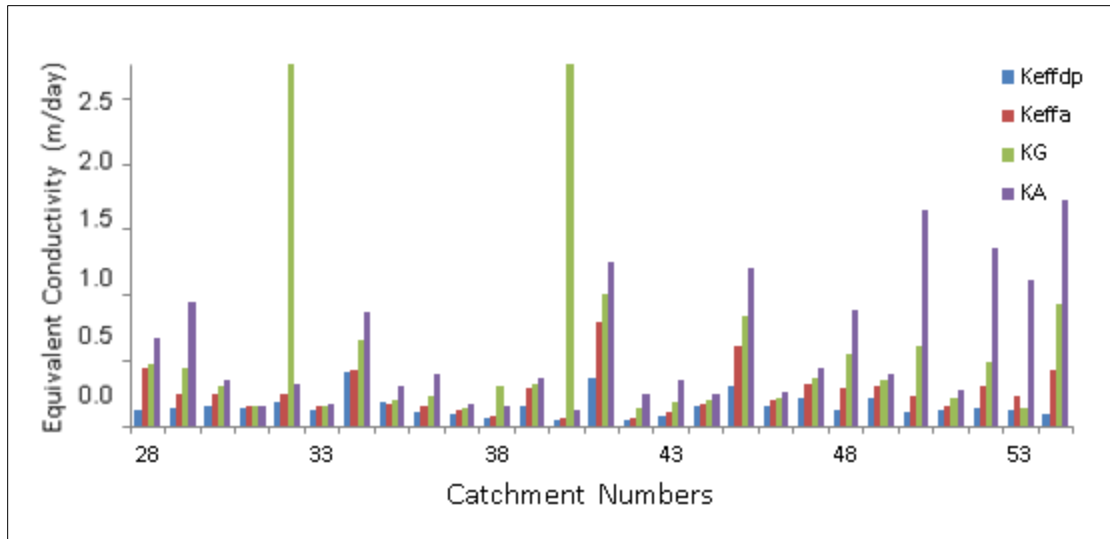


Figure 3.7. Catchment equivalent conductivity (m/day) estimated using the different approaches: $Kequiv_{dp}$, $Kequiv_a$, K_G and K_A for each of the 54 catchments. 28-53 represent the lower catchments of the watershed.

The study also investigated the equivalent conductivity along the major stream in the watershed, which is Oak Creek. Figure 3.8 shows the comparison of the $Kequiv_{mdp}$ (major drainage path) for Oak Creek stream and $Kequiv_a$ for the 12 corresponding catchments along Oak Creek stream. The average difference between $Kequiv_a$ for the 13 catchments and $Kequiv_{mdp}$ of Oak Creek was 0.005 m/day.

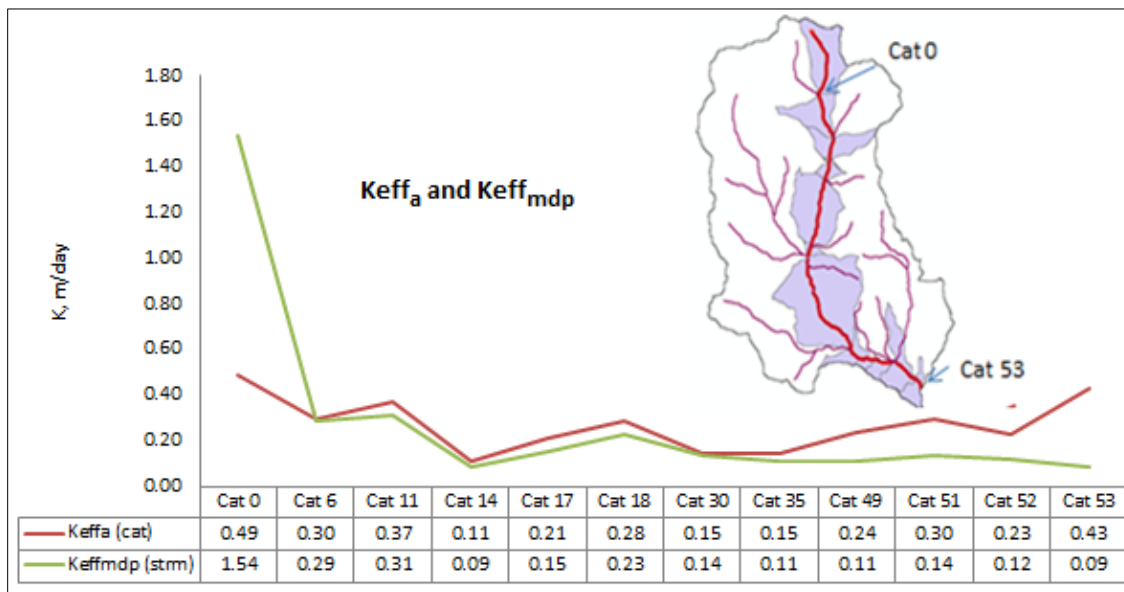


Figure 3.8. Equivalent conductivities along Oak Creek drainage path using the method of $Kequiv_{mdp}$ and equivalent conductivities of 12 catchments along Oak Creek drainage path using the method of $Kequiv_a$.

The descriptive statistics for the equivalent conductivities: K_A , K_G , $Kequiv_a$, $Kequiv_{dp}$, and $Kequiv_{mdp}$, for all the catchments in the watershed are shown in table 3.3. $Kequiv_{mdp}$ is included in table 3.3 but it is only within 12 of the 54 catchments in the watershed.

Table 3.3. Catchment descriptive statistics for equivalent conductivities (m/day): K_A , K_G , $Kequiv_a$, $Kequiv_{dp}$, and $Kequiv_{mdp}$.

	K_A	K_G	$Kequiv_a$	$Kequiv_{dp}$	$Kequiv_{mdp}$
Mean	1.04	0.62	0.38	0.31	0.28
Median	0.74	0.43	0.29	0.17	0.14
Mode	#N/A	0.09	#N/A	0.09	0.09
Std Dev.	1.06	0.59	0.32	0.35	0.40
Variance	1.11	0.34	0.10	0.12	0.16
Range	5.89	2.67	1.37	1.50	1.45
Min.	0.12	0.09	0.06	0.04	0.09
Max.	6.01	2.76	1.42	1.54	1.54
Count	54	54	54	54	12

The single equivalent conductivity values for the watershed are provided in table 3.4 from the five different methods: K_A , K_G , $Kequiv_a$, $Kequiv_{dp}$, $Kequiv_{mdp}$, and range from 1.16 to 0.16 m/day. The study's harmonic mean approach of using conductivity cell data from the entire watershed, from all drainage paths in the watershed or only cell values from the major drainage path – $Kequiv_a$, $Kequiv_{dp}$, and $Kequiv_{mdp}$, resulted in similar equivalent conductivity estimates. Even more unexpected, was that the same equivalent conductivity was calculated using the cell values in all of the drainage paths ($Kequiv_{dp}$) or using the cell values just in major drainage path ($Kequiv_{mdp}$) in the watershed. Both $Kequiv_{dp}$ and $Kequiv_{mdp}$ were 0.16 m/day for the watershed.

Table 3.4. Equivalent conductivity value for Oak Creek watershed

Kequiv, m/day	Method
1.16	K_A : standard arithmetic mean using all of the cell data in watershed
0.49	K_G : standard geometric mean (2D) using all cell data in watershed
0.24	$Kequiv_a$: new harmonic mean using all of the cell data in watershed
0.16	$Kequiv_{dp}$: new harmonic mean using all of the cell data in watershed's drainage paths
0.16	$Kequiv_{mdp}$: new harmonic mean using only the cell data in Oak Creek's drainage path

Discussion

The study presented a new method for calculating equivalent hydraulic conductivity from cell data with the use of GIS. The study's results calculated equivalent conductivities that support previous findings in literature: the arithmetic mean is greater than the geometric mean, which is greater than the harmonic mean or in this study $Kequiv_a$ (fig.3.6 and 3.7). It can be seen by comparing eqns. (1) and (2) that the equivalent conductivity determined from the arithmetic mean is determined mainly by layers or in this study, by cells, with the highest K values; whereas, the harmonic mean is mainly determined by cells with the lowest K values.

The study introduced for the first time, the comparison of equivalent conductivities for drainage paths, major and minor, to the equivalent conductivities of catchments and watersheds. The equivalent conductivities for catchments calculated by $Kequiv_a$, $Kequiv_{dp}$, and $Kequiv_{mdp}$ were all similar. Differences in catchment $Kequiv_a$ and catchment $Kequiv_{dp}$ and $Kequiv_{mdp}$ were due to the increased conductivity cell values in the feature. For example, in the upper reaches of the watershed where catchment 0 is located, the drainage path had larger conductivity cell values than in the corresponding cells in the catchment area, and in the lower reaches of the watershed, the drainage paths had lower conductivity cell values than corresponding cells in the catchment area.

Equivalent conductivities of the major drainage path in the watershed, Oak Creek stream, closely followed the equivalent conductivities for each corresponding catchment area with exception of catchment 0 and 53. Catchment 0 had a mixture of small, medium and high cell conductivities, but along Oak Creek stream drainage path in catchment 0, cell conductivities were high due to high soil infiltration properties. This resulted in a larger equivalent conductivity for the stream drainage outlet than the equivalent conductivity for the catchment. The opposite of this occurred in catchment 53, i.e., there were smaller conductivity cell values in the drainage path than conductivity cell values in the catchment. Overall, there is a decline in the equivalent conductivities $Kequiv_{dp}$ as the $Kequiv$ position in the watershed moves from the headwaters to the watershed outlet as shown in figure 3.8. This is because the upper reaches of the watershed probably have coarser and unsorted soils with steeper terrain compared to the lower reaches of the watershed have finer grained soils and flatter terrain.

The single equivalent conductivity for the entire watershed through evaluation of all the drainage paths is 0.16 m/day; through evaluation of just the major drainage path of Oak Creek stream it is 0.16 m/day; it is 0.24 m/day through evaluation of all the cells in the watershed; 0.49 m/day for the geometric mean; and 1.16 m/day for the arithmetic mean. Because the cell

conductivity values calculated in the study represent 1D horizontal flow, the equivalent geometric mean is not well-suited, since it represents equivalent conductivities for 2D flow. K_A and K_H are commonly used as upper and lower bounds to compare calculated equivalent hydraulic conductivity values and while $K_{equiv_{dp}}$ and $K_{equiv_{mdp}}$ are not within the lower bounds of K_{equiv_a} (this study's K_H) it is within reason to be plausible and to warrant further investigation.

The results from this study suggest that it is plausible that a single equivalent hydraulic conductivity for a watershed can be estimated using GIS methods from all the drainage paths in a watershed or from just the major drainage path in the watershed, as long as the drainage paths are representative of the conductivity values found in the catchments and watershed. Further investigation is required to see if similar results can be obtained from similar watersheds (topography, soils, precipitation, etc.) and across diverse watersheds.

Conclusion

A new technique was devised to calculate equivalent hydraulic conductivity, K_{equiv} with the use of GIS. The study demonstrated the use of GIS with both raster and vector data in the calculation of K_{equiv} . The new method was tested on irregularly shaped catchments as continuous data and on drainage paths represented as discrete vector data. The results showed that equivalent conductivity for a catchment or a watershed could be approximated from the conductivity values in the drainage paths. While this method is a local averaging approximation and not a robust nonlocal technique it does have its merits for one dimensional hydrological modeling.

Most upscaling techniques ignore elevation and slope. In this study, the results of the equivalent conductivities along *drainage paths* suggest that equivalent conductivity values decrease as the location moves from the headwaters to the watershed's outlet point and suggest further investigation could help to understand the role of these connected hydrologic features.

Hydraulic conductivity can vary in time and space. Field testing methods are time-consuming, costly, and result in point measurements which must be discretized and then calculated into an equivalent conductivity for the desired model scale. The technique of using drainage paths determined from high-resolution topography coupled with soil and precipitation utilizes the strengths of GIS and provides basin-wide hydraulic conductivity estimates which can then be upscaled.

Literature Cited

Arras, T. 2014. Manuscript in writing, Ph.D. Thesis, Oregon State University.

Bachu, S., and Cuthiell, D., 1990. Effects of core-scale heterogeneity on steady state and transient fluid flow in porous media: Numerical analysis, *Water Resource Research*, 26, 9-12.

Cardwell, W. T., and Parsons, R. L., 1945. Average permeabilities of heterogeneous oil sand. *The American Institute of Mining, Metallurgical and Petroleum Engineers*. P.34-42.

Dagan, Gedeon, 1993. Higher-order correction of effective permeability of heterogeneous isotropic formations of lognormal conductivity distribution. *Transport in Porous Media*, Vol. 12, Issue 3, 279-290.

Durlofsky, L.J., 1992. Representation of grid block permeability in coarse scale models of randomly heterogeneous porous media. *Water Resources Research*, 28, 1791-1800.

Freeze, R.A. and Cherry, J.A., 1979. *Groundwater*, Prentice-Hall, Inc. Englewood Cliffs.

Hashin, Z. and Shtrikman, S. 1962. *Journal of Applied Physics*. A variational approach to the theory of the effective magnetic permeability of multiphase materials. 33, 10, 3125.

Gomez-Hernandez, J.J. and Gorelick, S.M., 1989. Effective groundwater model parameter values: Influence of spatial variability of hydraulic conductivity, leakance and recharge. *Water Resources Research*, 25, 2331-2355.

Gutjahr, A.L., Gelhar, L.W., Bakr, A. A., and MacMillan, J.R., 1978. Stochastic analysis of spatial variability in subsurface flow: 2. Evolution and application. *Water Resources Research*, 14, 953-959.

Luo, W., Grudzinski, B. P., Pederson, D., 2010. Estimating hydraulic conductivity from drainage patterns: a case study in the Oregon Cascades. *Geology*, 38, 335–338.

Luo, W., Grudzinski, B. P., Pederson, D., 2011. Estimating hydraulic conductivity for the Martian subsurface based on drainage patterns: a case study in the Mare Tyrrhenum Quadrangle, *Geomorphology*, 125, 414–420.

Luo, W. and Pederson, D. T., 2012. Hydraulic conductivity of the High Plains Aquifer re-evaluated using surface drainage patterns. *Geophysical Research Letters*, 39, 1-6.

Luo, W., Stepinski, T.F., 2007. Topographically derived maps of valley networks and drainage density in the Mare Tyrrhenum quadrangle on Mars. *Geophysical Research Letters*, 33, 5-6.

Luo, W., Stepinski, T.F., 2008. Identification of geologic contrasts from landscape dissection pattern: an application to the Cascade Range, Oregon, USA. *Geomorphology*, 99, 90-98.

Journel, A. G., Deutsch, C.V., and Desbrats, A. J., 1986. Power averaging for block effective permeability. *Society of Petroleum Engineers*, 15128.

Maidment, David R., 2002. *ArcHydro: GIS for water resources*. ESRI, Inc.

Matheron, G., 1967. *Elements pour une theorie des milieux poreux*. Maisson et Cie.

Norman, S., P., 1992. Generalized scaling permeabilities: validation and effect of support scale. *Geophysical Research Letters*, 21 (5), 349-352.

Oosterbaan and Nijland, N.J. *Drainage Principles and Applications*. International Reclamation and Improvement; Manuscript 12, Determining the saturated hydraulic conductivity. www.waterlog.info. Publication 16, 2nd edition. 1994.

Renard, P. H., and Marsily, G., 1996. Calculating equivalent permeability: A review. *Advances in Water Resources*, 20, 253-278.

Surfleet, C. 2008. *Uncertainty in Forest Road Hydrologic Modeling and Catchment Scale: Assessment of Forest Road Sediment Yield*. Ph.D. Thesis, Oregon State University.

Tran, T., 1995. Addressing the missing scale: Direct simulation of effective modeling cell permeability. Tech. Rep. 8th annual meeting, Stanford Center for Reservoir Forecasting.

Vereecken, H., Kasteel, R., Vanderborght, J., and Harter, T., 2007. Upscaling hydraulic properties and soil water flow processes in heterogeneous soils: A review. *Vadose Zone Journal*, 6, 1 -28.

Vidstrand, P., 2001. Comparison of upscaling methods to estimate hydraulic conductivity. *Ground Water*, 39, No. 3, 401-407.

Wen, X-H. and Gomez-Hernandez, J.J., 1996. Upscaling hydraulic conductivities in heterogeneous media: An overview. *Journal of Hydrology*, 183, 1-2.

Yamada, T., 1995. A dissipation based on coarse grid system and its application to the scale-up of two phase problems. Tech. Report 8th annual meeting, Stanford Center for Reservoir Forecasting.

4. The Influence of DEM Resolution on Hydraulic Conductivity Values

Abstract

Over the last three decades, many authors have shown that increasing DEM resolution strongly influences computed hydrologic parameters. The majority of these studies have been conducted with 10 m and greater resolution DEMs and low-altitude aerial photography. Only recently have studies started to evaluate the utility of high-resolution DEMs obtained from airborne Light Detection and Ranging (LIDAR) for hydrologic investigations. The objective of this study was to investigate how calculated continuous hydraulic conductivity values and equivalent hydraulic conductivity values estimated with GIS are affected by DEM resolution. The study demonstrated that a 10 m DEM resolution is optimal when using GIS and landscape descriptors to estimate continuous conductivities and equivalent conductivities, when compared to 20 and 30 m DEM resolutions. While 20 and 30 m DEM resolutions appear suitable for these analyses there were underlying problems with accurate representation of channel depth and width with coarser DEMs.

Introduction

Topography dictates surface flow paths and is an important factor controlling the rate of water movement. Digital elevation models (DEMs) are used to represent topography and are being used to understand the hydrologic complexity and natural variability that occur across a landscape. DEMs are utilized for compiling watersheds, drainage areas, networked flow paths, and primary watershed characteristics, such as area, width, slope, profile and curvature (Beven and Moore, 1993). They are also being used for deriving secondary hydrologic attributes, which involve the combination of primary attributes to describe the spatial variability of the landscape through indices, such as, topographic wetness, stream power, terrain roughness, etc. (Moore et al., 1991; Wilson and Gallant, 2000).

Topography influences soil variability and terrain analysis has been developed as a quantitative method for predicting patterns of soil variability (McSweeney et al., 1994), regions of surface saturation (O'Loughlin, 1986; Moore et al., 1988), areas of erosion and deposition (Moore et al., 1988) and other hydrologic processes (Crave and Gascuel-Odoux, 1995; Gerla 1999). Numerous watershed hydrological models have incorporated spatial patterns of terrain, soils and vegetation (Band et al., 1991; 1993; Famiglietti and Wood, 1991; 1994; Moore and Grayson, 1991; Moore et al., 1993; Wigmosta et al., 1994). Lou et al (2010) and Arras and Istok (2014, manuscript in progress) have utilized DEMs with ancillary data to estimate basin-wide

continuous hydraulic conductivity values. Using DEMs to model landscape patterns has proven beneficial due to the ability to represent continuous properties across an entire landscape including areas not field sampled.

Previous studies have shown that, as the resolution of a DEM is decreased, slope steepness decreases, with greater differences in areas with steeper slopes (Chang and Tsai, 1991; Wolock and Price, 1994; Zang and Montgomery, 1994; Thielen et al., 1999). Total flow lengths and drainage density also decrease with decreased DEM resolution (Thielen et al., 1999; Wang and Yin 1998, Yin and Wang 1999). Wolock and Price (1994) demonstrated that upslope area is affected when DEM resolution is decreased. Zang and Montgomery (1994) suggested that for many landscapes a 10 m resolution is adequate for hydrologic modeling and increasing the resolution to 2 or 4 m does not provide additional information. Pradhan et al. (2006) demonstrated that the value of the topographic index, which is a spatial representation of the depth to water table and used in TOPMODEL (Beven et al., 1984), was strongly influenced by DEM resolution; as resolution increased, topographic index values increased, which was attributed to the loss of microtopography in the lower resolution DEM.

Over the last three decades, many authors have shown that increasing DEM resolution strongly influences computed hydrologic parameters. The majority of these studies have been conducted with 10 m and greater resolution DEMs and low-altitude aerial photography. Only recently have studies started to evaluate the utility of high-resolution DEMs obtained from airborne Light Detection and Ranging (LIDAR) for hydrologic investigations. With the advent of more accurate representations, is it possible to determine a range of suitable resolutions? Are derived topographic and hydrologic parameters for a 1 meter DEM similar to those derived for a 10 m DEM? What constitutes a model that is too computationally demanding for practical applications? To add to the complexity of the answer, technology to collect and process high-resolution data is constantly changing and improving. There is also the additional problem of high variability of model parameters within the landscape, such as hydraulic conductivity. Freeze (1980), Binley and Beven (1989) and Woolhiser et al. (1990) have demonstrated that the form of hillslope hydrographs is sensitive to the distribution of hydraulic conductivity. Progress has been made in estimating near-surface and profile soil water content with sensors and in the estimation of hydraulic conductivity (Entekhabi et al., 1985). However, soil hydraulic conductivity is still the least known of the land surface attributes (Nielson and Bourma, 1985) in comparison to topography and land cover which can be sampled remotely at high-resolutions from airborne or space borne platforms. The objective of this study was to investigate how hydraulic

conductivity and equivalent hydraulic conductivity values estimated from GIS are affected by DEM resolution.

Site Description

The study was performed on the Oak Creek watershed, a catchment in the Upper Willamette 8-digit Hydrologic Unit Code (17090003) subbasin, located in Benton County, OR. The Upper Willamette watershed is equivalent of the other Willamette basin watersheds (Yamhill, Tualatin, Middle Willamette, etc.) with respect to soils, topography, precipitation and climate. Oak Creek watershed is located in the McDonald/Dunn Research Forest managed by the College of Forestry, Oregon State University. The watershed area is ~ 3360 hectares; elevations range from 60 to more than 585 meters. The average annual precipitation for 1971-2000 was 137 cm/yr with a range of 107-188 cm/yr. Precipitation in the watershed is predominantly rain (~ 95 %). The underlying bedrock, the Siletz River Volcanics, is a basalt formation. The most common surface soil texture is silty clay loam, although some silty loam is also present. The forest trees are predominantly Douglas-fir with minor components of other conifers, hardwood species, and grassy meadows. There is a meteorological station near the outlet of the study watershed where continuous observations of air temperature, relative humidity, solar radiation, wind speed, and precipitation have been made since 2003. In addition, there are three rain gauges located in the watershed.

Methods

2010 LiDAR DEM was used for the delineation of Oak Creek's stream network and watersheds. LiDAR DEM data were obtained from Oregon Department of Geology and Mineral Industries (DOGAMI), in ESRI grid format with 1 m resolution. The 1 m DEM was resampled using cubic convolution resulting in resolutions of 10, 20, and 30 m. Horizontal hydraulic conductivity over the saturated thickness was estimated across Oak Creek watershed using LiDAR DEM and GIS. It is briefly reviewed here but for detailed discussion readers are referred to Arras and Istok (2014, manuscript in progress) and Lou et al. (2008, 2010, and 2011). The premise is based on Darcy's Law, which states

$$q = -K \frac{dh}{dl} \quad (1)$$

where q [LT^{-1}] is the volumetric groundwater flow rate per unit area (or flux); K [LT^{-1}] is the hydraulic conductivity; and dh/dl is the hydraulic gradient along the flow direction. Lou et al.

(2008, 2010, 2011) proposed methods to estimate hydraulic conductivity based on surface topography, flow path distances, recharge and aquifer thickness under the following assumptions: 1) the aquifer is equivalently drained (recharge equals discharge) and under steady-state dynamic equilibrium through the interplay of surface water, groundwater and topography and 2) groundwater flow is described by Darcy's Law, and the DuPuit-Forchheimer assumptions that the aquifer is unconfined and flow is primarily horizontal apply.

$$K = \frac{4W^2R}{[H^2 - (H - d)^2]} \quad (2)$$

where K is the hydraulic conductivity [L/T]; W is the length of equivalent groundwater drainage [L]; D is the drainage density [1/L]; R is the recharge rate [L/T]; d is the valley depth [L]; and H is aquifer thickness [L].

A 1 m DEM was used to delineate drainage paths based on a contributing area of 154 m² (0.038 acres), which resulted in 394 catchments within Oak Creek watershed. Aquifer thickness, H, was assumed constant (H = 98.4 m) in this study, based on estimates from USGS Scientific Investigations Report 2005-5168. The valley depth, d, was calculated with a Black Hat Transformation (BHT) using a focal statistics operation. In the previous study (Arras and Istok, 2014, manuscript in progress) the focal statistics operation used a radius of 4 cells for the 1 and 10 m DEMs. In this study a radius of 4 cells generated large valley depths which did not reflect true channel depths in the 30 m DEMs. As a result, the radius size was reduced to 3 cells from 4 cells in the 30 m DEM and a 4 cell radius was used with the 1, 10 and 20 m DEMs. Valley depth was averaged by catchment. Recharge, R, was estimated from precipitation and soil data (Arras and Istok, 2014, manuscript in progress; and Lou et. al., 2011). The 30-year (1971–2000) spatially variable mean annual precipitation data was obtained from Oregon State University, PRISM Climate Group. Soil Survey Geographic Database (SSURGO) was obtained from USDA-NRCS, and soil was assigned an infiltration percentage based on soil texture classification.

Equivalent conductivity was calculated using a new GIS approach of the harmonic mean for one dimensional horizontal flow. Readers are referred to Arras and Istok (2014, manuscript in progress) for detailed information; only a short review is provided here. Typically, equivalent conductivity for flow parallel to layers is calculated as a weighted arithmetic mean with each layer being treated as homogeneous. For flow perpendicular to layers, an equivalent conductivity value is calculated as a weighted harmonic mean. In this study, flow is parallel to

layers but moves through a heterogeneous layer of K values and uses a harmonic approach for calculation of $Kequiv$ for horizontal 1D flow (fig.4.1).

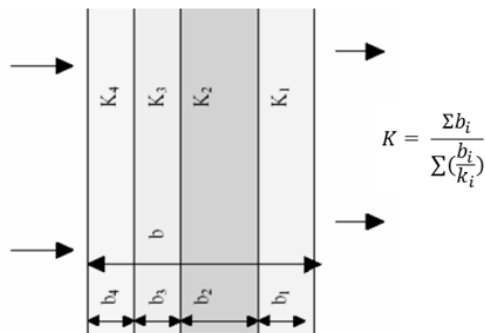


Figure 4.1. $Kequiv$, harmonic approach.

For discrete linear features, such as drainage paths, $Kequiv$, is calculated as:

$$Kequiv = \frac{\sum L_T}{\sum (L_{ki} / k_i)} \quad (3)$$

Where $Kequiv$ is the equivalent hydraulic conductivity, L_T is the total horizontal flow length being evaluated, L_{ki} is the horizontal length for each conductivity value and K is the conductivity value.

For areas represented with continuous data, such as catchments, $Kequiv$ is calculated as:

$$\frac{\sum (\text{no. grid cells in area})}{\sum (k_i \text{ no. cells} / k_i)} \quad (4)$$

In this study, $Kequiv$ for Oak Creek watershed was calculated using three different approaches:

1. $Kequiv_a$; using all the cells in the block area, such as a catchment or watershed

$$\frac{\sum (\text{no. cells in area})}{\sum (\text{no. cells of in } k_i \text{ area} / k_i)}$$
2. $Kequiv_{dp}$; using only the cells in the major and minor drainage paths

$$\frac{\sum (\text{no. cells in all drainage paths})}{\sum (\text{no. of cells in } k_i \text{ drainage paths} / k_i)}$$
3. $Kequiv_{mdp}$; using only the cells in the watershed's major drainage paths

$$\frac{\sum (\text{no. cells in major drainage paths})}{\sum (\text{no. of cells in } k_i \text{ drainage paths} / k_i)}$$

It is important to note that this study used a 1 m LiDAR DEM and coarsened DEMs and the authors' previous study used a 10 m USGS DEM. The two different DEM sources calculated slightly different hydraulic conductivity and equivalent conductivity values.

The study's conductivity values were compared to Krep values from the Soil Survey Geographic Database (SSURGO, 2009); calculated values from local pumping tests (Arras and Istok, 2014, manuscript in progress); and Surfleet's 2008 modeling study of Oak Creek watershed (Surfleet, PhD, Thesis, 2008). Surfleet's study included an estimate of saturated hydraulic conductivity at a stream gage in the watershed for water years 2005-2007. Surfleet quantitatively evaluated hydrologic model parameters in conjunction to stream flow and retained those parameters that exceeded a Nash Sutcliff Efficiency (NSE, Nash and Sutcliffe, 1970) threshold of 0.5. Surfleet estimated hydraulic conductivity values to range from 0.864 to 8,640 m/day for a NSE of 0.5 to 0.68 and for a NSE of \sim 0.68 (the highest in the study) conductivity values range from \sim 3 to 8 m/day. Surfleet's stream gage was located at N44.61° and W123.33°. After reviewing Surfleet's maps and using the relative location of roads and streams, the gage should be located along a 10 meter (35 ft) section of stream, roughly at N44.61° and W123.33°. This 10 m stream segment was buffered 5 m on both sides and the study's conductivity values were averaged inside the buffered area for comparison to Surfleet's values.

Results

The descriptive statistics for the original 1 m LiDAR DEM and for the coarsened 10, 20 and 30 m DEMs after resampling indicated that as DEM resolutions are coarsened, minimum elevation values increase and maximum elevation values decrease. This agrees with previous findings that coarsening of DEM resolution using a cubic convolution resampling acts as a "smoothing" process. The maximum slope value drops sharply from 77.44° to 39.84° and mean slope values decrease gradually as resolutions are coarsened as the DEM resolution decreases from 1 to 30 m.

Table 4.1 Watershed DEM statistics, feet.

DEM Resolution	Max	Min	Mean	Std Dev
1 m	2162.47	248.98	761.60	382.53
10 m	2161.81	250.45	761.16	382.17
20 m	2158.81	250.51	762.42	383.07
30 m	2158.95	252.06	762.09	382.95

Slope (%)

DEM Resolution	Max	Min	Mean	Std Dev
1 m	75.44	0	13.94	9.05
10 m	44.16	0.19	13.01	8.26
20 m	41.27	0.02	12.44	7.89
30 m	39.84	0.03	11.95	7.58

Figure 4.2. shows Oak Creek watershed, pumping test locations, stream gage location and three transects across drainage channels in the upper, middle, and lower areas of the watershed. Figure 4.3 shows the difference in elevation between the 1 m LiDAR DEM and the resampled 10, 20 , and 30 m DEMs along each transect. It can be seen that there is reasonable agreement between the DEMs in the flat areas and a much larger difference in the channel areas of the terrain. The channel in the lower transect is roughly 30 feet wide by 10 feet deep; one channel side has a moderate slope and the surrounding terrain is relatively flat. The channel in the middle transect is a well-defined deep and narrow channel, about 20 feet wide by 10 feet deep; and the upper transect channel is gently sloping on both sides with no distinct side channel boundaries or depth. Comparing channel depth for the 1 m LiDAR DEM to the 10, 20, and 30 m DEMs show the general trend of decreasing channel depth. In the middle transect, the 30 m DEM reduced the channel depth less than the 20 m DEM, which was unexpected and probably the result of the neighboring cells in the resampling algorithm. The maximum channel depth difference from the 1 m LiDAR DEM to each coarsened DEM occurred in the 30 m DEM for the lower and upper watershed transects, and in the 20 m DEM for the mid watershed transect.

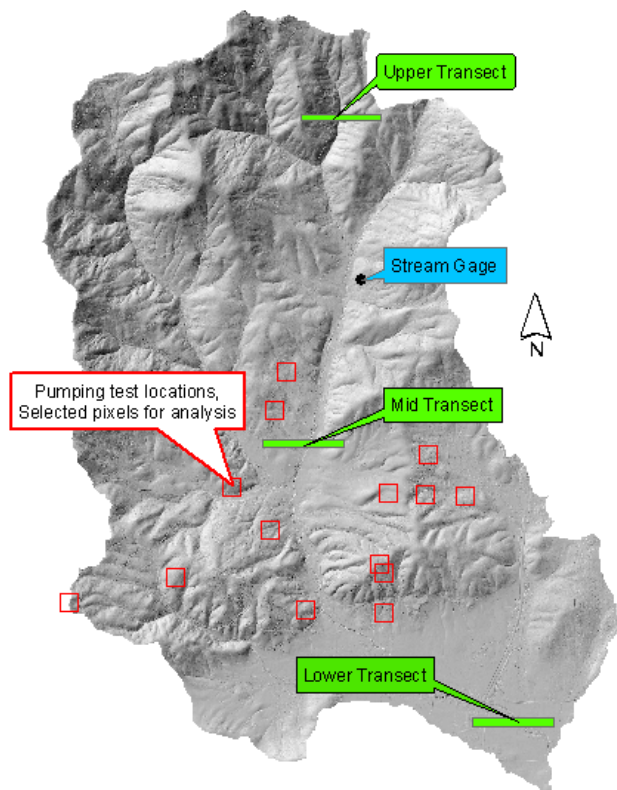


Figure 4.2. Oak Creek watershed study area, location of pumping tests, stream gage, and transects.

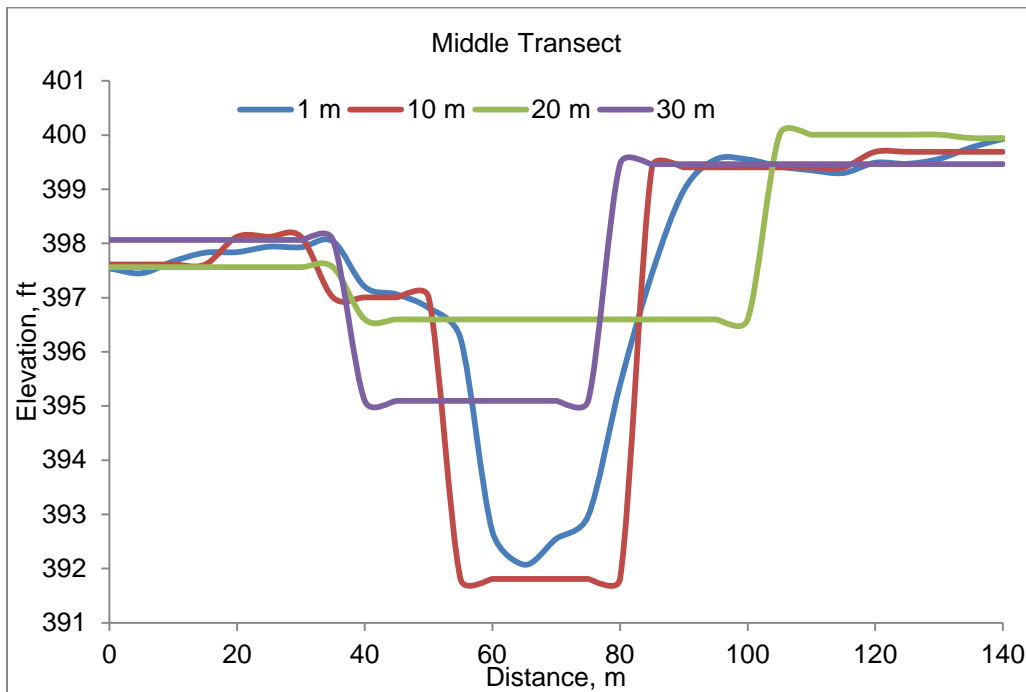
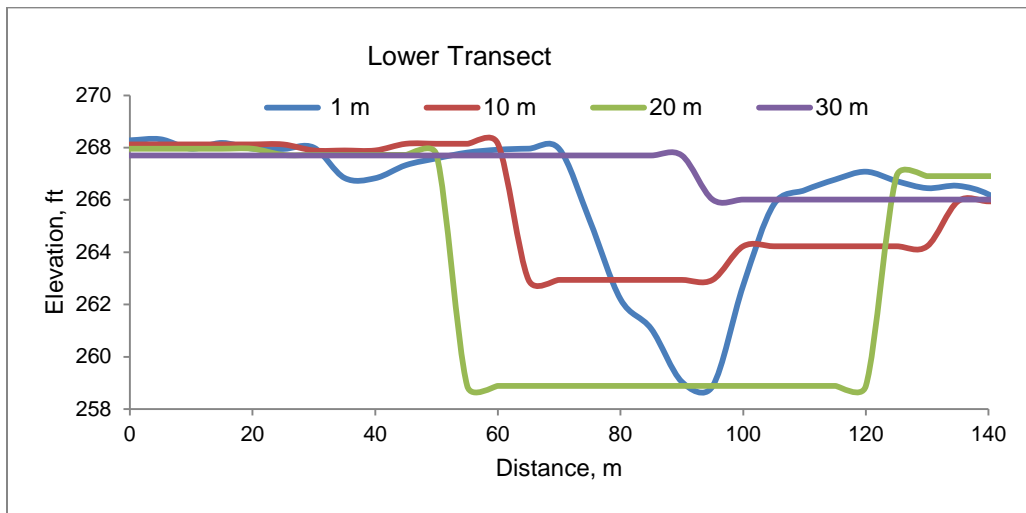
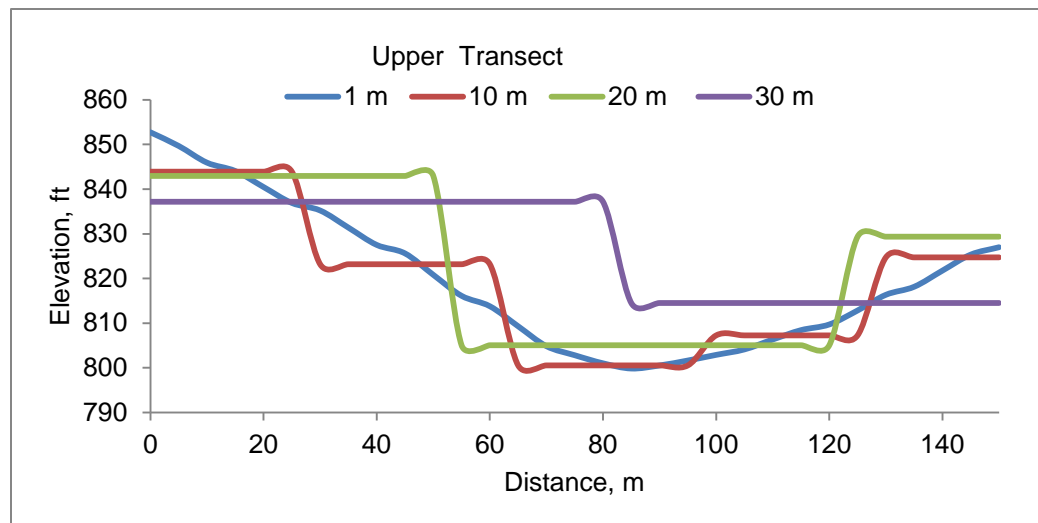


Figure 4.3. Channel cross-sections and tables showing difference between 1 m LiDAR DEM and coarsened 10, 20, and 30 m DEMs for lower, middle and upper transects.



Lower Transect			Middle Transect			Upper Transect		
DEM Resolution	Minimum Elevation (feet)	Elevation Difference from 1 m DEM (feet)	DEM Resolution	Minimum Elevation, (feet)	Elevation Difference from 1 m DEM, (feet)	DEM Resolution	Minimum Elevation (feet)	Elevation Difference from 1 m DEM (feet)
1 m	258.87	0.00	1 m	392.07	0.00	1 m	799.83	0.00
10 m	262.94	4.07	10 m	391.81	-0.26	10 m	800.53	0.70
20 m	258.89	0.02	20 m	396.60	4.53	20 m	805.04	5.21
30 m	266.01	7.14	30 m	395.10	3.02	30 m	814.50	14.67

Cont. Figure 4.3. Channel cross-sections and tables showing difference between 1 m LiDAR DEM and coarsened 10, 20, and 30 m DEMs for lower, middle and upper transects.

As expected, decreasing the resolution of a DEM created a smoother, less defined landscape, with more moderate slopes and lower values of channel depth, d . However, the average channel depth per catchment surprisingly increased as resolutions were coarsened with an increase in the maximum, mean, and standard deviation as resolutions are coarsened (Figure 4.4). The largest averaged channel depths occur in the 30 m DEM. Even though channel depths became smaller in coarsened DEMs, the BHT process, which was used to calculate channel depth, produced larger channel depth values as resolution increased. The BHT process uses a focal statistic operation, in which a roving window of a user-defined array of cells is used to evaluate a selected statistic (maximum, minimum, etc.) in the window. The result of the evaluated statistic is the new output cell value, and then the roving window moves to next cell and the process is repeated. In this study, a 3 x 3 (i.e., 3 rows by 3 columns) window was used for the 1, 10 and 20 m DEMs and a 4 x 4 window was used for the 30 m DEM. The BHT is started by determining the maximum elevation in the 3x3 roving window of the DEM; the output of this process is called dilation. The operation is repeated but the input layer is now the dilation

layer and the minimum cell value is used as the statistic. The output result of this is a closing layer. The last step in determining the channel depth is to subtract the DEM from the closing layer and then to average channel depths by catchment.

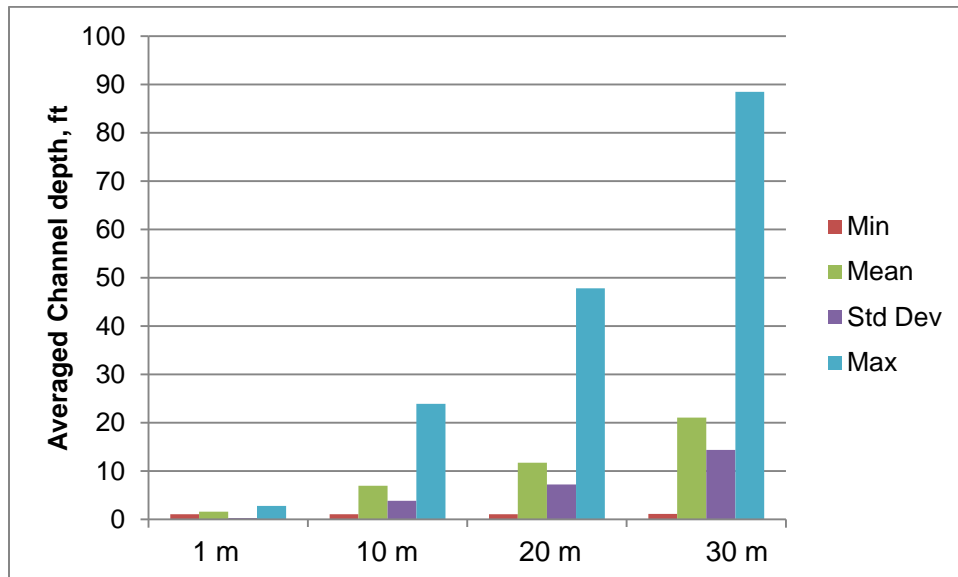
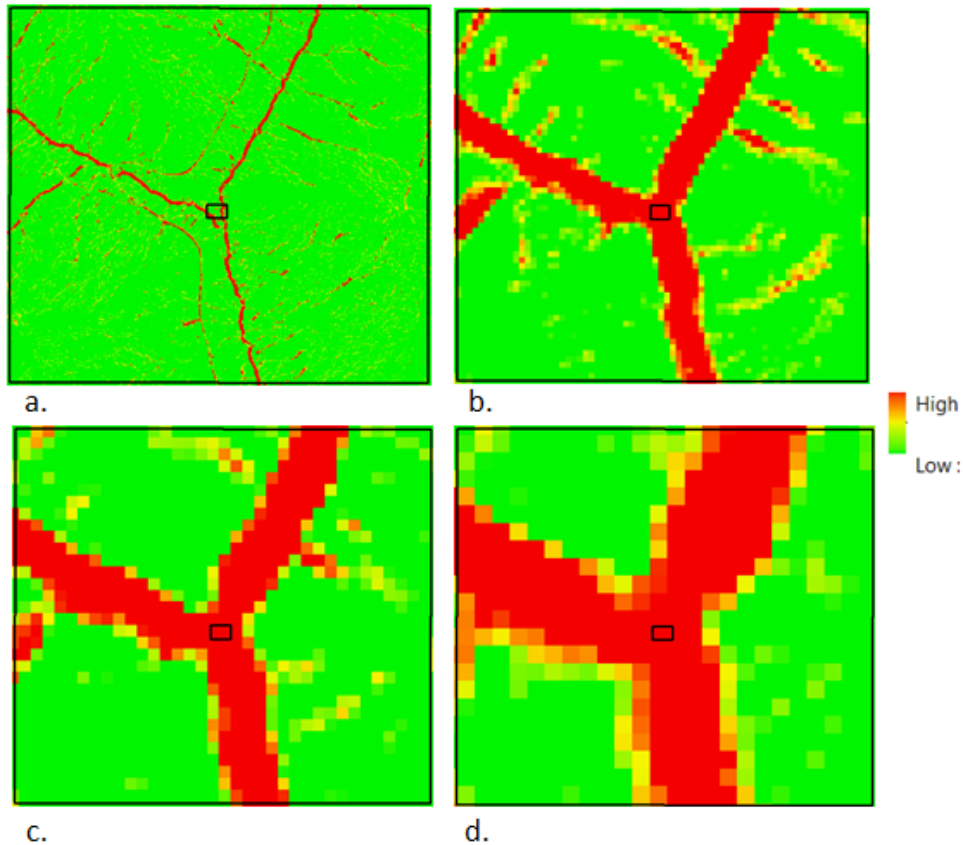


Figure 4.4. Averaged catchment channel depth statistics for 1 m LiDAR DEM, coarsened 10 m, 20 m, and 30 m DEMs (after the Black Hat Transformation).

A small area of 0.45 km² (112 acres) was investigated to understand how elevation, BHT dilation, BHT closing, BHT channel depth and averaged channel depth by catchment changed in the coarsened DEMs (Figure 4.5). In the 1 m LiDAR DEM, BHT channel depth is small and narrow, and as the DEM resolution is coarsened, channel depth increases, as well as, widens. The table in figure 4.5; provides the center cell value (center of the smaller rectangle) of each processing step in calculating the average channel depth by catchment. Figure 4.6 shows a hillshade of the area.



Cell measurements taken within small rectangle	1 m (a.)	10 m (b.)	20 m (c.)	30 m (d.)
Elevation, ft	663	670.84	664.95	667.53
BHT Dilation, ft	666.08	706.87	742.23	819.47
BHT Closing, ft	664.28	699.32	724.1	787.72
BHT Channel depth, ft	1.28	28.48	59.15	120.19
BHT Average Channel depth by catchment, ft	1.68	13.91	26.99	50.83

Figure 4.5. Cell values for BHT processed layers (ft), for: a. 1 m LiDAR DEM, b. 10 m DEM, c. 20 m DEM, and d. 30 m DEM. The numbers in the table correspond to the small rectangle shown in the center of each panel.

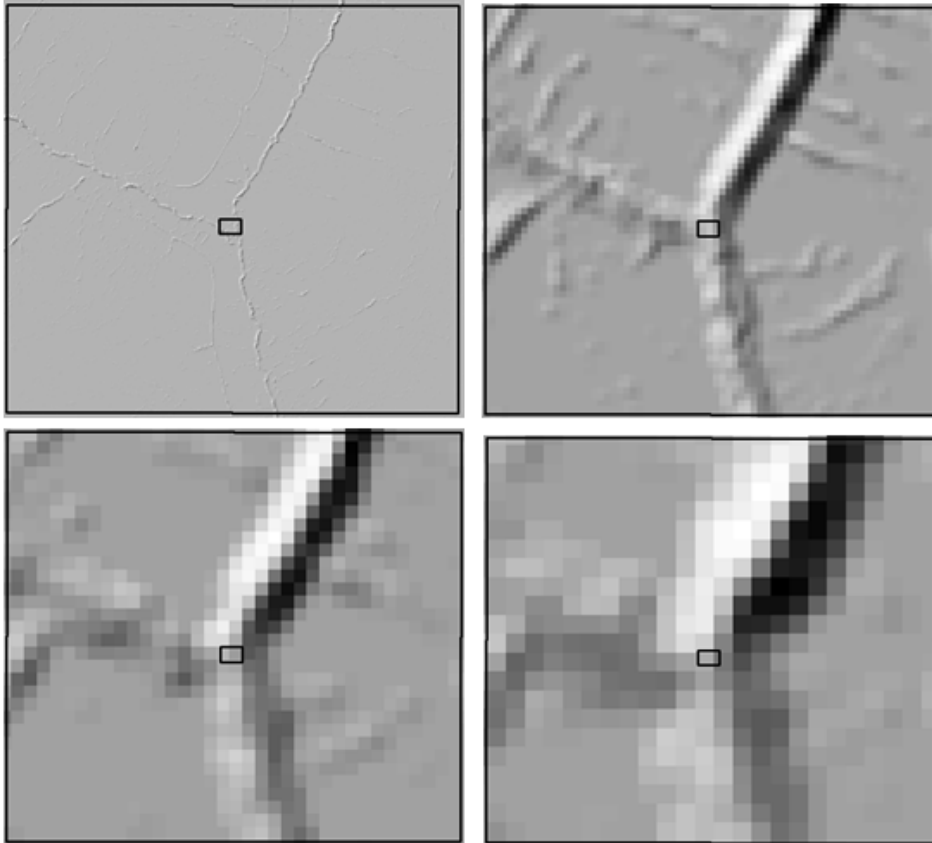


Figure 4.6. Hillshade of BHT channel depth (small test area). Top left image is 1 m LiDAR DEM; top right, 10 m DEM; bottom left, 20 M DEM; and bottom right, 30 m DEM.

Channel depth, as determined by the BHT, increases as DEM resolution is coarsened and this becomes critical because a critical parameter in the calculation of hydraulic conductivity in this study is channel depth. The most prominent differences among the DEM resolutions were the differences of drainage paths and channel depths.

Hydraulic conductivity was calculated for Oak Creek watershed for all DEM resolutions. As shown in table 4.2, conductivity values decrease from 1 to 10 to 20 m DEMs and conductivities substantially increase in the 30 m DEM.

Table 4.2. Descriptive Statistics of K for Oak Creek watershed across resolutions.

K, m/day	1 m Radius 4 cells	10 m Radius 4 cells	20 m Radius 4 cells	30 m Radius 3 cells
Min	0.0007	0.0002	0.008	0.003
Max	62.02	16.82	14.67	741.74
Mean	4.48	1.29	0.83	33.96
STD Dev.	6.98	2.10	1.40	66.72

The conductivity values computed using the four DEM resolutions were compared to K values computed from pumping test data, soil survey K_{rep} values, and Surfleet's study (table 4.3). The positional location of the pumping tests was estimated by Miles (2011) to be within a few meters; the worst case scenario, the location of the pumping tests could be within +/- 10 m (32 ft). A 10 m buffer was created around each pumping test location and conductivity values were averaged in the buffered area. Table 4.4 and table 4.5 provide the differences between the study's conductivity values and the soil survey, K_{rep} , and the pumping tests K values. The 10 m DEM has the smallest standard deviation when compared to the soil survey data and the 20 m DEM has the smallest standard deviation when compared to the pumping test K values. The 30 m DEM has the largest standard deviation when compared to both the soil survey data and the pumping tests.

Table 4.3. K (m/day) estimates at pumping test locations and Surfleet's stream gage: soil survey data, pumping tests and the calculated K from this study.

Object ID	OR Well Start No.	Soil Survey 2009	Pumping tests	1 m	10 m	20 m	30 m	Surfleet's K
1	143834	0.78	0.24	0.65	0.17	0.11	4.71	-
2	131820	0.78	0.58	0.33	0.09	0.05	1.23	-
3	131817	0.78	0.09	0.33	0.09	0.05	1.22	-
4	128523	0.08	3.05E-05	1.58	0.37	0.25	13.02	-
5	127774	0.78	9.14E-05	0.81	0.41	0.28	14.62	-
6	83887	19.65	0.12	10.10	1.65	1.13	50.35	-
7	107079	0.78	0.24	0.67	0.12	0.08	2.57	-
8	67490	0.78	0.46	0.52	0.11	0.08	4.38	-
9	63838	0.78	1.83	0.52	0.13	0.08	3.24	-
10	54727	0.78	3.05E-05	0.82	0.21	0.10	3.19	-
11	44103	0.78	3.05E-05	1.70	0.53	0.35	14.56	-
12	33803	0.78	1.55	0.16	0.11	0.04	1.49	-
13	144876	0.78	1.58	0.95	0.26	0.18	8.25	-
14	Surfleet	0.78	-	0.46	0.13	0.10	1.5	3-8

Table 4.4. Conductivity (m/day) differences between soil survey, Krep, and the study's values at different DEM resolutions.

OR Well	Δ Diff. (soil K_{rep} -1 m)	Δ Diff. (soil K_{rep} -10 m)	Δ Diff. (soil K_{rep} -20 m)	Δ Diff. (soil K_{rep} -30 m)
143834	0.13	0.61	0.67	-3.93
131820	0.45	0.69	0.73	-0.45
131817	0.45	0.69	0.73	-0.44
128523	-1.5	-0.29	-0.17	-12.94
127774	-0.03	0.37	0.5	-13.84
83887	9.55	18	18.52	-30.7
107079	0.11	0.66	0.7	-1.79
67490	0.26	0.67	0.7	-3.6
63838	0.26	0.65	0.7	-2.46
54727	-0.04	0.57	0.68	-2.41
44103	-0.92	0.25	0.43	-13.78
33803	0.62	0.67	0.74	-0.71
144876	-0.17	0.52	0.6	-7.47
Surfleet	0.32	0.65	0.68	-0.72
Std Dev.	3.87	3.57	3.58	10.05
*Std Dev.	0.57	0.27	0.24	5.03

*without 83887

Table 4.5. Conductivity differences between pumping tests and the study's values at different DEM resolutions, m/day.

OR Well	Δ Diff. (pumping K-1 m)	Δ Diff. (pumping K-10 m)	Δ Diff. (pumping k-20 m)	Δ Diff. (pumping k-30 m)
143834	-0.41	0.07	0.13	-4.47
131820	0.25	0.49	0.53	-0.65
131817	-0.24	0	0.04	-1.13
128523	-1.58	-0.37	-0.25	-13.02
127774	-0.81	-0.41	-0.28	-14.62
83887	-9.98	-1.53	-1.01	-50.23
107079	-0.43	0.12	0.16	-2.33
67490	-0.06	0.35	0.38	-3.92
63838	1.31	1.7	1.75	-1.41
54727	-0.82	-0.21	-0.10	-3.19
44103	-1.70	-0.53	-0.35	-14.56
33803	1.39	1.44	1.51	0.06
144876	0.63	1.32	1.4	-6.67
Std Dev.	1.91	0.55	0.52	10.07

Three equivalent conductivity values for the Oak Creek watershed were estimated using the raster and vector $Kequiv$ methods, reference Arras and Istok (2014, manuscript in progress), reference Table 4.6. $Kequiv_a$ used all cells in the watershed, $Kequiv_{dp}$ used all drainage paths cells in the watershed and $Kequiv_{mdp}$ used only the major drainage path cells, Oak Creek stream, in the watershed. The 20 m resolution produced similar equivalent conductivity values regardless of the method. The 10 m resolution calculated similar equivalent conductivity values for $Kequiv_a$ and $Kequiv_{mdp}$ and the 20 m resolution had similar $Kequiv_{dp}$ and $Kequiv_{mdp}$. The 30 m resolution had the largest range of equivalent conductivity values.

Table 4.6. Equivalent conductivity ($Kequiv$), m/day for Oak Creek Watershed.

	1 m	10 m	20 m	30 m
$Kequiv_a$	0.91	0.25	0.17	5.03
$Kequiv_{dp}$	0.59	0.11	0.12	4.00
$Kequiv_{mdp}$	0.44	0.20	0.12	0.84

Discussion

Because the drainage density remained the same in all of the DEM resolutions investigated, $4W^2R$ (eqn 2) remained constant in all the models. H , aquifer thickness, also remained constant, at 98.4 m (30 ft). The only parameter to change in each model was channel depth, d . As the resolution of DEMs increased, microtopography was lost and the channel depth was reduced. However, the Black Hat Transformation process produced larger channel depths as DEM resolutions were coarsened. The channel depth was averaged by catchment and became larger than the aquifer thickness and resulted in negative K values across many catchments. This became problematic in the 20 m and 30 m DEM models and was resolved by using a smaller radius window during the focal statistics operation. The 1, 10, and 20 m DEMs used a 4 cell window in the focal statistics operation and the 30 m DEM used a 3 cell window. Lou et al., 2010, conducted a similar study in the Oregon Cascades with a 37.315 meter DEM and did not indicate this was a problem. However, their study used an aquifer thickness of 500 m, compared to an aquifer thickness of 98.4 m in Oak Creek and Lou et al., used a different Black Hat Transformation algorithm.

Hydraulic conductivity values across Oak Creek watershed decrease with increasing DEM resolution until the DEM resolution coarsened to 30 m and then K increase significantly. The 1 m DEM has a larger range of conductivities than compared to the 10 and 20 m DEMs,

and the 10 and 20 m DEMs have comparable conductivity statistics. The standard deviation suggests the 10 m DEM provides the most similar values to the soil survey data at the pumping test locations and also similar to the 20 and the 1 m DEM; while the 20 m DEM resolution conductivity values are most similar to the pumping tests.

Oak Creek's equivalent conductivity values for the watershed range from 0.91 - 0.44 m/day at the 1 m resolution, 0.25-0.11 m/day for 10 m, 0.17 – 0.12 m/day for 20 m, and 5.03- 0.84 m/day for 30 m. It was unexpected how similar the equivalent conductivity values were for the 10 m and 20 m resolution DEMs. The data suggest as the resolutions move from the very fine resolution (1 m) to coarser resolutions (10 and 20 m) the equivalent conductivities decrease until 30 m, then the values increase beyond the pattern of the other resolutions. The data suggest that an equivalent conductivity for Oak Creek watershed can be estimated using all the cells in the watershed, the cells in all the drainage paths or just the cells from the major drainage path.

As the resolution of a DEM drops below the necessary resolution to capture the significant patterns of the surface, the underlying model that explicitly routes water cannot be used. Cell resolution defines flow width and channel depth and this reflected the basic problem of the 30 m DEM in this study and to some extent the 20 m DEM. Although, the 20 and 30 m resolution could not precisely describe the channel depth or width to be used with confidence within the context of the GIS method used in this study, the estimated conductivity results are still plausible. However, understanding how channel depth is reduced by the 20 and 30 m DEM and how the BHT exaggerates the channel depth neither resolutions are recommend for use in these methods. If an improved method of estimating channel depth could be utilized in coarser DEMs then the methods could be useful. Last, there is also a lack of accuracy in two of the study's variables - aquifer thickness and soil infiltration, which contributes to the uncertainty of the results but aquifer thickness is not a sensitive parameter in the model and the best data available at the time was used in the study. Recent advances in remote sensing and soil mapping should provide improved soil data.

Conclusion

The objective of this study was to investigate how continuous hydraulic conductivity values and equivalent conductivity values estimated with GIS are affected by DEM resolution. The study demonstrated that 1, 10 and 20 m DEM resolutions result in similar conductivity and similar equivalent conductivity estimates for the watershed. With LiDAR DEM becoming more common, additional studies should investigate the differences elevations, channel depths, and

slopes between LiDAR DEMs and other DEM sources. For watershed modeling purposes, a 1 or 10-meter DEM is recommended for estimating continuous with GIS. The 10 DEMs produced similar results as the 20 m DEM but lacks detailed information in channels. A 20 m and 30 m DEMs are only recommended for this method if an improved method to determine average channel depth per catchment can be incorporated and especially if a study area has shallow aquifer depths.

Can an equivalent hydraulic conductivity value for a watershed be estimated across DEM resolutions? The results suggest that it can. All of the calculated equivalent conductivity values are plausible. However, since the methods are heavily dependent on the accurate description of the topography the authors have greater confidence in the 1 and 10 m DEM.

The question of an optimal resolution remains to be answered and greatly depends on the variable of interest and the properties of the landscape. In the Oak Creek watershed, a 1 or a 10 m DEM appears to be optimal for estimating continuous conductivity values across the watershed but 1 m DEMs are also data intensive and LiDAR DEMs are not widely available to date. With the ease of computing, and data storage in mind, a 10 m DEM is more efficient than a 1 m DEM and 10 m DEMs are widely available.

Literature Cited

Arras, T. 2014. Manuscript in writing, Ph.D. Thesis, Oregon State University.

Band, L.E., 1991. Distributed parameterization of complex terrain. In Wood, E. F. (Ed.), *Land Surface-Atmosphere Interactions for Climate Modeling*. Kluwer Academic, Dordrecht. 249-270.

Band, L.E., Moore, I.D., 1995. Scale – landscape attributes and geographical information-systems. *Hydrological Processes*, 9, 3–4, 401–422.

Band, L.E., Patterson, P., Nemani, R., Running, S.W., 1993. Forest ecosystem processes at the watershed scale – incorporating hillslope hydrology. *Agricultural and Forest Meteorology* 63 (1–2), 93–126.

Beven, K. J., 1984. Runoff production and flood frequency in catchment of order n: An alternative approach in *Scale Problems in Hydrology*, edited by V. K. Gupta et al., 107-131,

Beven, K. J. 1989. 'Changing ideas in hydrology - The case of physically-based models', *Journal of Hydrology*, 105, 157-172.

Beven, K.J., Moore, I.D., 1993. *Terrain Analysis and Distributed Modeling in Hydrology*. Wiley, New York.

Binley, A. and Beven, K. 1989. A physically based model of heterogeneous hillslopes: Equivalent hydraulic conductivities, *Water Resources Research*, 25, 1227-1233.

- Chang, K.T., Tsai, B.W., 1991. The effect of DEM resolution on slope and aspect mapping. *Cartographic Geographic Information Systems*, 18, 69–77.
- Crave, A., Gascuel-Oudou, C., 1995. The influence of topography on time and space distribution of soil water content. *Hydrological Processes*, 11, 203–210.
- Entekhabi, D., Nakamura, H. and Njoku, E. G. 1994. Solving the inverse problem for soil moisture and temperature profiles by sequential assimilation of multifrequency remotely sensed observations', *IEEE Trans. Geoscience Remote Sensing*, 32, 438-448.
- Famiglietti, J. S. and Wood, E. F., 1991, Evapotranspiration and Runoff from Large Land Areas: Land Surface Hydrology for Atmospheric General Circulation Models, *Surveys in Geophysics*, 12, 179-204.
- Famiglietti, J. S. and Wood, E. F., 1994, Multi-Scale Modeling of Spatially-Variable Water and Energy Balance Processes, *Water Resources Research*, 30(11), 3061-3078.
- Freeze, R. A. 1980. A stochastic-conceptual analysis of rainfall runoff processes on a hillslope. *Water Resources*, 16, 391-408.
- Gerla, P.J., 1999. Estimating the ground-water contribution in wetlands using modeling and digital terrain analysis. *Wetlands* 19, 394–402.
- Luo, W., Grudzinski, B. P., Pederson, D., 2010. Estimating hydraulic conductivity from drainage patterns: a case study in the Oregon Cascades. *Geology*, 38, 335–338.
- Luo, W., Grudzinski, B. P., Pederson, D., 2011. Estimating hydraulic conductivity for the Martian subsurface based on drainage patterns: a case study in the Mare Tyrrhenum Quadrangle, *Geomorphology* 125, 414–420.
- Luo, W., Stepinski, T.F., 2008. Identification of geologic contrasts from landscape dissection pattern: an application to the Cascade Range, Oregon, USA. *Geomorphology*, 99, 90-98.
- McSweeney, K.M., Gessler, P.E., Slater, B., Hammer, R.D., Bell, J.C., Petersen, G.W., 1994. Towards a new framework for modeling the soil-landscape continuum. In: Amundson, R.G. Ed., *Factors of Soil Formation: A Fiftieth Anniversary Retrospective*. SSSA Spec. Publ. 33. Soil Science Society American Journal, Madison, WI, 127–145.
- Moore, I., D., Gessler, P.A, Nielsen, Peterson, 1993. Soil attribute prediction using terrain analysis. *Soil Science Society American Journal*, 57, 443-452.
- Moore, I.D., Grayson, R.B., Ladson, A.R., 1991. Digital terrain modeling: a review of hydrological, geomorphologic and biological applications. *Hydrological Processes*, 5, 3–30.
- Moore, I.D., O'Loughlin, E.M., Burch, G.J., 1988. A contour-based topographic model for hydrological and ecological applications. *Earth Surfaces Processes Landforms*, 13, 305–320.
- Nash, J. E. and Sutcliffe, J. V. 1970. River flow forecasting through conceptual models. 1. A discussion of principles, *Journal of Hydrology*, 10, 282-290.

Nielsen, D. R. and Bouma, J. 1985. Soil spatial variability. In Proceedings of a Workshop of the International Soil Science Society and the Soil Science Society of America. Pudoc, Wageningen, 243.

O'Loughlin, E.M., 1986. Prediction of surface saturation zones in natural catchments by topographic analysis. *Water Resource Resources*, 22, 5, 794–804.

Pradhan, N. R., Y. Tachikawa, and K. Takara (2006), A downscaling method of topographic index distribution for matching the scales of model application and parameter identification, *Hydrological Processes*, 20(6), 1385–1405.

Saulnier, G-M, Obled, C. O, Beven K., 1997. Analytical compensation between DTM grid resolution and the equivalent values of saturated hydraulic conductivity within topmodel framework. *Hydrological Processes*, Vol. 11, 1331-1346.

Surfleet, C. 2008. Uncertainty in Forest Road Hydrologic Modeling and Catchment Scale: Assessment of Forest Road Sediment Yield. Ph.D. Thesis, Oregon State University.

Thieken, A.H., Lucke, A., Diekkruger, B., Richter, O., 1999. Scaling input data by GIS for hydrological modeling. *Hydrological Processes*, 13, 611–630.

Quinn, P. F., Beven, K. J. and Lamb, R. (1995), The $\ln(a/\tan\beta)$ index: How to calculate it and how to use it within the topmodel framework. *Hydrology Processes*, 9, 161–182.

Wang, X., Yin, Z.-Y. et al., 1998. A comparison of drainage networks derived from digital elevation models at two scales. *Journal of Hydrology*, 210, 221–241.

Wigmosta, M. S., Vail, L. W., and Lettenmaier, D. P. 1994. A distributed hydrology-vegetation model for complex terrain. *Water Resources Research*, 30, 1665-1679.

Wilson, J.P., Repetto, P.L., Snyder, R.D., 2000. Effect of data source, grid resolution and flow-routing method on computed topographic attributes. In: Wilson, J.P., Gallant, J.C. (Eds.), *Terrain Analysis: Principles and Applications*. John Wiley and Sons, New York, 133–161.

Wolock, D. M. and Price, C. V. 1994. Effects of digital elevation model map scale and data resolution on a topography-based watershed model. *Water Resource Research*, 30, 3041-3052.

Woolhiser, D.A., and Goodrich, D. C., 1988. Effect of storm rainfall intensity patterns on surface runoff, *J. Hydro.*, 102, 335--354.

Yin, Z.-Y., Wang, X., 1999. A cross-scale comparison of drainage basin characteristics derived from digital elevation models. *Earth Surfaces Processes Landforms*, 24, 557–562.

Zhang, W. and Montgomery, D. R. 1994. Digital elevation model grid size, landscape representation and hydrologic simulations. *Water Resources Research*, 30, 1019-1028.

Conclusion

The importance of this research lies with using GIS for improving the hydraulic conductivity estimates that are used for many water resource modeling efforts, including predicting the transport of pollutants in ground water, computing surface runoff for flood control, and computing water budgets. Hydraulic conductivity can be experimentally determined in the laboratory or in the field and both are time consuming, expensive to collect, subject to various sampling and testing artifacts, and sparse. Laboratory and field methods provide point estimates of hydraulic conductivity and are prone to scaling problems when discretized across an entire basin. Conventional interpolation methods, such as kriging have been used to estimate continuous basin-scale values of hydraulic conductivity and while these methods are valuable they lack the utilization of landscape descriptors such as slope, soil infiltration, and groundwater depth. The interaction between topography, surface water, and aquifer properties have long been recognized but literature is limited on hydraulic conductivity studies with the fusion of geomorphology (Lou and Pederson, 2011).

The ability to utilize the strengths of GIS coupled with high-definition topography and landscape data to estimate continuous conductivity values for any defined hydrologic area is significant. The United States Department of Agriculture, Natural Resources Conservation Service provides digital soil data of the United States, which contains representative hydraulic conductivity estimates for each soil unit boundary. Conductivity estimates are produced by observation of ancillary data (aerial photography, geology, vegetation, etc.) and soil characteristics. These soil attributes are incorporated into an implicit conceptual model that is used to infer soil variation and is applied to predict soil variation at unobserved sites. The soil data are then transferred on aerial photographs by soil unit boundaries. Soil survey hydraulic conductivity values are represented as a single value across a soil unit map boundary (one K value for an entire soil polygon). The final product of the soil survey have unknown assumptions, limitations, accuracy and is heavily dependent on the knowledge of the soil surveyor (Hewitt, 1993). While the soil survey data has been severely criticized in the scientific community, it is the single largest soil data source available to date. From this research, it is conceivable to envision a published digital soil data layer of continuous (raster) hydraulic conductivity values across the United States at a resolution of 10m. This would be significant. While this method certainly requires further testing, the methodology does have known assumptions, accuracy could be assessed, and limitations could be developed.

The concept of using GIS to estimate equivalent conductivity has been presented for the first time and exploits the power of GIS. Both the study's conductivity and equivalent conductivity values were plausible and agreed with published soil data, pumping tests, and one independent study conducted in the study's watershed. However, the study's findings also revealed that while conductivity values from 1, 10, 20 and 30 m DEMs appear similar and even plausible there were problems with coarser DEMs. As DEM resolutions were coarsened channel depths were reduced and investigation revealed that estimated channel depths actually increased due to the processing technique utilized. This led to the identification that the model breaks at DEM resolutions of 20 and 30m because channel depths become larger than the aquifer depth and result in negative conductivity values.

The implications of the study's results have the potential of developing new theories connecting hydraulic conductivity and equivalent conductivity to geomorphology and detailed landscape descriptors. While this study provided evidence that contributes to the knowledge and understanding that it is plausible to use GIS and geomorphology to estimate continuous conductivity values and equivalent values in a watershed additional research still needs to be conducted. The study identified that accurate drainage density is an important characteristic of the model, as is channel depth; both of which lead to additional questions. Can an improved automated technique be utilized to determine channel depth? Can accurate drainage delineation and channel depth from a highly descriptive DEM (LiDAR) be applied to a coarser DEM for hydraulic conductivity estimation? Can the study's techniques be applied in watersheds where the topography is flat? Can equivalent conductivity values be estimated from drainage paths in other diverse watersheds? Since the resolution of a 1m DEM goes beyond the level of detail of most published conductivity values (soil data) could field tests be conducted in the study's watershed to evaluate the accuracy of a 1m DEM for estimating conductivity and equivalent conductivity values using these methodologies? While many more questions could be addressed these are the ones at the forefront.

Literature Cited

Burrough, P.A., Beckett, P.H. and Jarvis, M.G. 1971. The relation between cost and utility in soil survey. *Journal of Soil Science*, 22, 368-81.

Hewitt, A.E. 1993: Predictive modelling in soil survey. *Soil and Fertilizers*, 56, 305–14.

Luo, W. and Pederson, D. T., 2012. Hydraulic conductivity of the High Plains Aquifer re-evaluated using surface drainage patterns. *Geophysical Research Letters*, 39, 1-6.

5. Bibliography

- Arras, T. 2014. Manuscript in writing, Ph.D. Thesis, Oregon State University.
- Bachu, S., and Cuthiell, D., 1990. Effects of core-scale heterogeneity on steady state and transient fluid flow in porous media: Numerical analysis, *Water Resource Research*, 26, 9-12.
- Band et al., 1991. Distributed parameterization of complex terrain. In Wood. E. F. (Ed.), *Land Surface-Atmosphere Interactions for Climate Modeling*. Kluwer Academic, Dordrecht. 249-270.
- Band, L.E., Moore, I.D., 1995. Scale – landscape attributes and geographical information-systems. *Hydrological Processes*, 9, 3–4, 401–422.
- Band, L.E., Patterson, P., Nemani, R., Running, S.W., 1993. Forest ecosystem processes at the watershed scale – incorporating hillslope hydrology. *Agricultural and Forest Meteorology* 63 (1–2), 93–126.
- Beven, K .J., 1984. Runoff production and flood frequency in catchment of order n: An alternative approach in *Scale Problems in Hydrology*, edited by V. K. Gupta et al., 107-131,
- Beven, K. J. 1989. 'Changing ideas in hydrology - The case of physically-based models', *Journal of Hydrology*, 105, 157-172.
- Beven, K.J., Moore, I.D., 1993. *Terrain Analysis and Distributed Modeling in Hydrology*. Wiley, New York.
- Binley, A. and Beven, K. 1989. A physically based model of heterogeneous hillslopes: Equivalent hydraulic conductivities, *Water Resources Research*, 25, 1227-1233.
- Burrough, P.A., Beckett, P.H. and Jarvis, M.G. 1971. The relation between cost and utility in soil survey. *Journal of Soil Science*, 22, 368-81.
- Cardwell, W. T., and Parsons, R. L ., 1945. Average permeabilities of heterogeneous oil sand. *The American Institute of Mining, Metallurgical and Petroleum Engineers*. P.34-42.
- Chang, K.T., Tsai, B.W., 1991. The effect of DEM resolution on slope and aspect mapping. *Cartographic Geographic Information Systems*, 18, 69–77.
- Conlon, T. D, Wozniak, K. C., Woodcock, D., Herrera, N. B., Fisher, B. J., Morgan, D. S., Lee, K. K, Hinkle, S. R., 2005. *Ground-Water Hydrology of the Willamette Basin, Oregon*. USGS, Scientific Report 2005-5168.
- Crave, A., Gascuel-Oudou, C., 1995. The influence of topography on time and space distribution of soil water content. *Hydrological Processes*, 11, 203–210.
- Dagan, Gedeon, 1993. Higher-order correction of effective permeability of heterogeneous isotropic formations of lognormal conductivity distribution. *Transport in Porous Media*, Vol. 12, Issue 3, 279-290.

Domenico, P. A., Schwartz, F. W., 1990. *Physical and Chemical Hydrogeology*. Wiley & sons, New Jersey.

Durlafsky, L.J., 1992. Representation of grid block permeability in coarse scale models of randomly heterogeneous porous media. *Water Resources Research*, 28, 1791-1800.

Entekhabi, D., Nakamura, H. and Njoku, E. G. 1994. Solving the inverse problem for soil moisture and temperature profiles by sequential assimilation of multifrequency remotely sensed observations', *IEEE Trans. Geoscience Remote Sensing*, 32, 438-448.

Famiglietti, J. S. and Wood, E. F., 1991, Evapotranspiration and Runoff from Large Land Areas: Land Surface Hydrology for Atmospheric General Circulation Models, *Surveys in Geophysics*, 12, 179-204.

Famiglietti, J. S. and Wood, E. F., 1994, Multi-Scale Modeling of Spatially-Variable Water and Energy Balance Processes, *Water Resources Research*, 30(11), 3061-3078.

Fotheringham, A. S., and Rogerson, P. A., 1994. *Spatial Analysis and GIS*. Taylor & Francis, London.

Freeze, R.A. and Cherry, J.A., 1979. *Groundwater*, Prentice-Hall, Inc. Englewood Cliffs.

Freeze, R. A. 1980. A stochastic-conceptual analysis of rainfall runoff processes on a hillslope. *Water Resources*, 16, 391-408.

Gerla, P.J., 1999. Estimating the ground-water contribution in wetlands using modeling and digital terrain analysis. *Wetlands* 19, 394-402.

Gomez-Hernandez, J.J. and Gorelick, S.M., 1989. Effective groundwater model parameter values: Influence of spatial variability of hydraulic conductivity, leakance and recharge. *Water Resources Research*, 25, 2331-2355.

Goodchild, M. F., 1992. Geographical information science. *International Journal of Geographical Information Systems*, 6, 31-45.

Goodchild, M. F., Parks, B. O., Steyaert, L.T., Johnston, 1996. *GIS and Environmental Modeling: Progress and Research Issues*. John Wiley & Sons, New Jersey.

Gupta, N., Rudra, R.P., and Parkin, G. Analysis of spatial variability of hydraulic conductivity at field scales. *Canadian Biosystems Engineering*, 48, 1.55-1.62.

Gurnell, A.M., and Montgomery, D.R, 2000. *Advances in Hydrologic Processes: Hydrological Applications of GIS*. John Wiley & Sons, New York.

Gutjahr, A.L., Gelhar, L.W., Bakr, A. A., and MacMillan, J.R., 1978. Stochastic analysis of spatial variability in subsurface flow: 2. Evolution and application. *Water Resources Research*, 14, 953-959.

- Hashin, Z. and Shtrikman, S. 1962. Journal of Applied Physics. A variation-al approach to the theory of the effective magnetic permeability of multiphase materials. 33, 10, 3125.
- Hewitt, A.E. 1993: Predictive modelling in soil survey. Soil and Fertilizers, 56, 305–14.
- Jha, M.K., Chowdhury, A., Chowdary, V.M., Peiffer, S. 2007. Groundwater management and development by integrated remote sensing and geographic information system: prospects and constraints. Water Resources Management, 21, 427-467.
- Journel, A. G., Deutsch, C.V., and Desbrats, A. J., 1986. Power averaging for block effective permeability. Society of Petroleum Engineers, 15128.
- Lagacherie, P., McBratney, A.B., Voltz, M., Digital Soil Mapping An Introductory Perspective. - Developments in Soil Science Series, Elsevier Publisher, Ch. 43.
- Lee, K. K. and Risley, J.C., 2002. Estimates of Ground-Water Recharge, Base Flow and Stream-Reach Gains and Losses in the Willamette River Basin, Oregon. USGS, Portland, Oregon.
- Luo, W., Grudzinski, B. P., Pederson, D., 2010. Estimating hydraulic conductivity from drainage patterns: a case study in the Oregon Cascades. Geology, 38, 335–338.
- Luo, W., Grudzinski, B. P., Pederson, D., 2011. Estimating hydraulic conductivity for the Martian subsurface based on drainage patterns: a case study in the Mare Tyrrhenum Quadrangle, Geomorphology 125, 414–420.
- Luo, W., Stepinski, T.F., 2007. Topographically derived maps of valley networks and drainage density in the Mare Tyrrhenum quadrangle on Mars. Geophysical Research Letters, 33, 5-6.
- Luo, W., Stepinski, T.F., 2008. Identification of geologic contrasts from landscape dissection pattern: an application to the Cascade Range, Oregon, USA. Geomorphology, 99, 90-98.
- Luo, W. and Pederson, D. T., 2012. Hydraulic conductivity of the High Plains Aquifer re-evaluated using surface drainage patterns. Geophysical Research Letters, 39, 1-6.
- Maidment, D. R., Goodchild, M. F., Parks, B. O., Steyaert, L. T. (Eds.). 1993. GIS and hydrologic modeling. In: Environmental Modeling with GIS. Oxford Press Univ. Press, NY, 147-167.
- Maidment, David R., 2002. ArcHydro: GIS for water resources. ESRI, Inc.
- Manning, C. E., and Ingebritsen, S. E., 1999, Permeability of the continental crust: constraints from heat flow models and metamorphic systems. Reviews in Geophysics, 37, 127-150.
- Matheron, G., 1967. Elements pour une theorie des milieux poreux. Maisson et Cie.
- McDonnell, R. A., 1996. Including the spatial dimension: using geographical information systems in hydrology. Progress in Physical Geography, 20, 159-177.

- McElwee, C. D. (1980), Theis Parameter Evaluation from Pumping Tests by Sensitivity Analysis. *Ground Water*, 18, 56–60.
- McSweeney, K.M., Gessler, P.E., Slater, B., Hammer, R.D., Bell, J.C., Petersen, G.W., 1994. Towards a new framework for modeling the soil-landscape continuum. In: Amundson, R.G. Ed., *Factors of Soil Formation: A Fiftieth Anniversary Retrospective*. SSSA Spec. Publ. 33. Soil Science Society American Journal, Madison, WI, 127–145.
- Miles, Evans (2011). A GIS Study of Benton County, Oregon, Groundwater: Spatial Distributions of Selected Hydrogeologic Parameters, Oregon State University.
- Montgomery, D.R., Dietrich, W.E., 1989. Source areas, drainage density, and channel initiation. *Water Resources Research*, 25, 1907–1918.
- Montgomery, D.R., Dietrich, W.E., 1992. Channel initiation and the problem of landscape scale. *Science* 255 (5046), 826–829.
- Moore, I., D., Gessler, P.A, Nielsen, Peterson, 1993. Soil attribute prediction using terrain analysis. *Soil Science Society American Journal*, 57, 443-452.
- Moore, I.D., Grayson, R.B., Ladson, A.R., 1991. Digital terrain modeling: a review of hydrological, geomorphologic and biological applications. *Hydrological Processes*, 5, 3–30.
- Moore, I.D., O’Loughlin, E.M., Burch, G.J., 1988. A contour-based topographic model for hydrological and ecological applications. *Earth Surfaces Processes Landforms*, 13, 305–320.
- Nash, J. E. and Sutcliffe, J. V. 1970. River flow forecasting through conceptual models. 1. A discussion of principles, *Journal of Hydrology*, 10, 282-290.
- Neuman, S., 1990. Universal scaling of hydraulic conductivities and dispersivities in geologic media. *Water Resources Research* 26, 1749–1758.
- Neuman, S., 1994. Generalized scaling of permeabilities: validation and effect of support scale. *Geophysical Research Letters*, 21, 349–352.
- Nielsen, D. R. and Bouma, J. 1985. Soil spatial variability. In *Proceedings of a Workshop of the International Soil Science Society and the Soil Science Society of America*. Pudoc, Wageningen, 243.
- Norman, S., P., 1992. Generalized scaling permeabilities: validation and effect of support scale. *Geophysical Research Letters*, 21 (5), 349-352.
- O’Loughlin, E.M., 1986. Prediction of surface saturation zones in natural catchments by topographic analysis. *Water Resource Resources*, 22, 5, 794–804.
- Oosterbaan and Nijland, N.J. *Drainage Principles and Applications*. International Reclamation and Improvement; Manuscript 12, Determining the saturated hydraulic conductivity. www.waterlog.info. Publication 16, 2nd edition. 1994.

Peucker, T.K., Douglas, D.H., 1975. Detection of surface-specific points by local parallel processing of discrete terrain elevation data. *Computer Graphics and Image Processing*, 4, 375–387.

Phillips, O.M., 2003. Groundwater flow patterns in extensive shallow aquifers with gentle relief: Theory and application to the Galena/Locust Grove region of eastern Maryland. *Water Resources Research*, 39, 1149-1163.

Pradhan, N. R., Y. Tachikawa, and K. Takara (2006), A downscaling method of topographic index distribution for matching the scales of model application and parameter identification, *Hydrological Processes*, 20(6), 1385–1405.

Refsgaars, J.C., Hojberg, A.L., Moller, I., Hansen, M., Sondergaard, V., 2010. Groundwater modeling in integrated water resources management – visions for 2020. *Groundwater*, 48, 633-648.

Renard, P. H., and Marsily, G., 1996. Calculating equivalent permeability: A review. *Advances in Water Resources*, 20, 253-278.

Rigon, Riccardo; Rodriguez-Iturbe, Ignacio; Maritan, Amos; Giacometti, Achille; Tarboton, David; and Rinaldo, Andrea, 1996. On Hack's Law. *Water Resources Research*, 32. 3367-3374.

Rodriguez-Iturbe, I., Rinaldo, A., 1997. *Fractal River Basins: Chance and Self-Organization*. Cambridge Univ. Press, New York.

Sánchez-Vila, X. Girardi, J. P., Carrera, J., 1995. A Synthesis of Approaches to Upscaling of Hydraulic Conductivities. *Water Resources Research*, 31, 867-882.

Saulnier, G-M, Obled, C. O, Beven K., 1997. Analytical compensation between DTM grid resolution and the equivalent values of saturated hydraulic conductivity within topmodel framework. *Hydrological Processes*, Vol. 11, 1331-1346.

Surfleet, C. 2008. *Uncertainty in Forest Road Hydrologic Modeling and Catchment Scale: Assessment of Forest Road Sediment Yield*. Ph.D. Thesis, Oregon State University.

Tarboton, D.G., 1997. A new method for the determination of flow directions and upslope areas in grid digital elevation models. *Water Resources Research*, 33, 309-319.

Tarboton, D.G., Ames, D.P., 2001. Advances in the mapping of flow networks from digital elevation data. *World Water and Environmental Resources Congress*. ASCE, Orlando, Florida.

Thielen, A.H., Lucke, A., Diekkruger, B., Richter, O., 1999. Scaling input data by GIS for hydrological modeling. *Hydrological Processes*, 13, 611–630.

Tran, T., 1995. Addressing the missing scale: Direct simulation of effective modeling cell permeability. Tech. Rep. 8th annual meeting, Stanford Center for Reservoir Forecasting.

Tucker, G.E., Catani, F., Rinaldo, A., Bras, R.L., 2001. Statistical analysis of drainage density from digital terrain data. *Geomorphology*, 36, 187–202.

Quinn, P. F., Beven, K. J. and Lamb, R. (1995), The $\ln(a/\tan\beta)$ index: How to calculate it and how to use it within the topmodel framework. *Hydrology Processes*, 9, 161–182.

USDA, NRCS, Soil Survey of Benton County, Oregon. 2009.

Vereecken, H., Kasteel, R., Vanderborght, J., and Harter, T., 2007. Upscaling hydraulic properties and soil water flow processes in heterogeneous soils: A review. *Vadose Zone Journal*, 6, 1 -28.

Vidstrand, P., 2001. Comparison of upscaling methods to estimate hydraulic conductivity. *Ground Water*, 39, No. 3, 401-407.

Wang, X., Yin, Z.-Y. et al., 1998. A comparison of drainage networks derived from digital elevation models at two scales. *Journal of Hydrology*, 210, 221–241.

Wen, X-H. and Gomez-Hernandez, J.J., 1996. Upscaling hydraulic conductivities in heterogeneous media: An overview. *Journal of Hydrology*, 183, 1-2.

Wigmosta, M. S., Vail, L. W., and Lettenmaier, D. P. 1994. A distributed hydrology-vegetation model for complex terrain. *Water Resources Research*, 30, 1665-1679.

Wilson, J.P., Repetto, P.L., Snyder, R.D., 2000. Effect of data source, grid resolution and flow-routing method on computed topographic attributes. In: Wilson, J.P., Gallant, J.C. (Eds.), *Terrain Analysis: Principles and Applications*. John Wiley and Sons, New York, 133–161.

Wolock, D. M. and Price, C. V. 1994. Effects of digital elevation model map scale and data resolution on a topography-based watershed model. *Water Resource Research*, 30, 3041-3052.

Woolhiser, D.A., and Goodrich, D. C., 1988. Effect of storm rainfall intensity patterns on surface runoff , *J. Hydro.*, 102, 335--354.

Yamada, T., 1995. A dissipation based on coarse grid system and its application to the scale-up of two phase problems. Tech. Report 8th annual meeting, Stanford Center for Reservoir Forecasting.

Yin, Z.-Y., Wang, X., 1999. A cross-scale comparison of drainage basin characteristics derived from digital elevation models. *Earth Surfaces Processes Landforms*, 24, 557–562.

Zhang, W. and Montgomery, D. R. 1994. Digital elevation model grid size, landscape representation and hydrologic simulations. *Water Resources Research*, 30, 1019-1028.